Add textspanish{} to all spanish words, phrases, and passages

Check accents in all spanish

Phenological Classification of Crops in Northwest Argentina Using 250-meter MODIS

Imagery

by

Jarrett Alexander Keifer

A thesis submitted in partial fulfillment of the
requirements for the degree of

Master of Art
in
Geography

Thesis Committee:
Jiunn-Der Duh, Chair
David Banis
Leopoldo Rodriguez

Portland State University
2014

ABSTRACT

Subtropical deforestation in Latin America is thought to be driven by demand for agricultural land, particularly to grow soybeans. However, existing remote sensing methods that can differentiate crop types to verify this hypothesis require high spatial or spectral resolution data, or extensive ground truth information to develop training sites, none of which are freely available for much of the world. Here, I propose a new method of crop classification using multi-temporal MODIS vegetation indices as a base image from which to extract crops using their phenologies. I test and refine this method in Kansas, USA using the USDA crop data layer as reference. I then test the applicability of the method to other regions of the world by applying it to data from Pellegrini, Santiago Del Estero, Argentina. The study is to examine if using phenological profiles in image classification is a viable method to verify the initial hypothesis that soybeans are driving deforestation in subtropical South America.

Something fancy.

Acknowledgements

Something goes here.

Contents

List of Tables

List of Figures

Todo list

Chapter 1

Introduction

Deforestation has long been a concern throughout tropical South America. However, this process of land use/land cover (LULC) change from forest to other uses has been increasingly recognized in subtropical South America as a significant source of environmental degradation. Understanding the complex dynamics of subtropical deforestation is crucial given the prominent role of forests in debates about climate change, conservation, and the protection of endangered species (Geist and Lambin 2002; Zak, Cabido, and Hodgson 2004; Bonnie 2000; Houghton 1994; Sala et al. 2000).

Currently, many perceive growing demand for agricultural land—particularly land for soybeans—to be one of the greatest pressures on South American subtropical forests (Pengue 2005; Grau, Gasparri, and Aide 2005; Altieri and Pengue 2006). Remote sensing has given researchers a tool to classify land cover and measure deforestation, but the often used multi-spectral or multi-temporal image classification techniques require extensive ground truth information for the accurate classification of common crop types using widely-available data. Therefore, getting a complete picture of the dynamics of deforestation, including an under-

standing of agricultural pressures on forests, requires rarely-available high spatial or high

spectral resolution data (Senay et al. 2000) or expensive field time gathering training site

data. The development of a tool that can efficiently and effectively extract crop types using

widely-available imagery would be of value to the field.

The primary goal of this thesis is to develop and test a phenological classification toolset

that can identify and extract crop types from a multi-date vegetation index sequence assem-

bled using free and accessible data from the National Aeronautics and Space Administra-

tion's (NASA) Moderate Resolution Imaging Spectroradiometer (MODIS) platform. The

toolset is tested in Kansas, USA using the U.S. Department of Agriculture's (USDA) crop

data layer (CDL) as ground truth to derive reference temporal signatures of summer crops

and to test the accuracy of the classifier. Using the Kansas-derived reference signatures,

imagery of the 2014 summer growing season in the Department of Pellegrini, Santiago del

Estero, Argentina (Fig. 1.1) is classified to examine the toolset's applicability in subtropical

South America.

Figure 1.1: The department of Pellegrini, Santiago Del Estero, Argentina.

Chapter 2

Background

Deforestation and the *Ley de Bosques* (Forest Act) in Argentina

The conversion of forestland to other uses has seriously impacted Argentina's forests. In 1915 it was remarked that 30 percent of the country had forest cover, but in 2001 only 10 percent remained forested (Secretaría de Desarrollo Sustentable y Política Ambiental [Argentina] 2001). Over the period 1998 to 2002, Argentina lost over 940,000 hectares of forest cover (Secretaría de Ambiente y Desarrollo Sustentable [Argentina] 2007). The high rate of deforestation concerned policymakers, and Law 26.331, or the *Ley de Bosques* (Forest Act), was voted into law in 2007 in an effort to preserve remaining native forests. Areas of native forest are defined to be those with forest cover of at least 20 percent native species, and that have trees of a minimum of 7 meters high. The law designates red, yellow, and green areas, each with different restrictions on clearing and use. Red is assigned to areas of "high conservation value," yellow is for areas that must be managed sustainably, and green allows "partial or total use" (Gulezian 2009: 25). Each provincial government was responsible

for determining how to classify their native forest area, and each enacted the *Ley de Bosques* regulations under the *Ordenamiento Territorial de los Bosques Nativos* (Land Management Order for Native Forests, OTBN).

As a part of Law 26.331 ongoing land cover studies are done to examine the effectiveness of the legislation. Between 2006 and the passing of the law, 573,296 hectares of native forest cover were lost. From the passing of the law in 2007 and the classification of the OTBN areas in 2009, a further 473,001 hectares were deforested. From the enacting of the OTBN (in 2009) and 2011, some 459,108 hectares were found to have been lost (Secretería de Ambiente y Desarrollo Sustentable [Argentina] 2012). This suggests that, in the context of the native forest areas, the *Ley de Bosques* may have had a small effect in reducing deforestation, but overall levels still remain quite high. This has led some to question the effectiveness of the law at slowing cutting (Valpreda 2012; Greenpeace Argentina 2013), and calls for a better understanding of the driving forces of deforestation in Argentina.

Soy and its effects

The increase of soybean in Argentina has occurred at a rapid pace throughout the last two decades, making it the third largest producer of soy in the world (US Foreign Agricultural Service 2013). Necessarily, as soy production rises, so does its spatial extent and the intensity of cultivation methods. Currently, almost all of Argentina's soy production is using genetically modified (GM) varieties, specifically Monsanto's "Roundup Ready" beans (Greenpeace International 2005). The highly mechanized and input intensive nature of this

crop type calls into question other environmental consequences of soybean cultivation, such as pesticide runoff, glyphosate-resistant weeds, and soil depletion (Pengue 2005).

A number of studies have addressed soy and deforestation in Northwest Argentina, but only one has used methods capable of mapping crop types in deforested areas (Volante et al. 2005). However, this study by the Argentine *Instituto Nacional de Tecnología Agropecuraia* (National Institute of Agricultural Technology, INTA) does not have well-documented methodology and has not been updated since 2005. Of the remainder, all used remote sensing techniques to classify only LULC and not specific crop types, leaving the effect of soy on LULC as an underlying assumption (Grau, Gasparri, and Aide 2005; Grau, Aide, and Gasparri 2005; Grau, Gasparri, and Aide 2008; Boletta et al. 2006; Gasparri and Grau 2009). While the extreme deforestation in Argentina is undeniable—and certainly soy plays a part—its role has not been examined in full, leaving unsubstantiated the perception of soy as the driving force in this process.

The goal of this research is to develop an image classification capable of mapping agricultural crops by type, allowing soy to be explicitly identified on remotely sensed imagery. The accurate and efficient mapping of soy distributions and their changes over time could allow further investigation of the roles of soy in deforestation. The direct and indirect effects soy crops have had on deforestation can thus be understood conceptually and systemically at both regional and local scales, which could lead to the development of more effective policies for land management (Brown et al. 2007).

Chapter 3

Study Areas

This study will use agricultural areas in Kansas, USA for testing and verification of the phenological classification method and will apply the classification method to Pellegrini, Santiago del Estero, Argentina to test its effectiveness in subtropical South America.

3.1   Kansas, USA

The state of Kansas is one of the big agricultural producers of the US. As one of the plains states, it is relatively flat across much of its extent, making it well suited to large highly-mechanized agro-industrial operations. In 2012, the three most extensive crops in the state were wheat, corn, and soybeans (Table 3.1), which are also the most abundant crops in Pellegrini, Argentina. Additionally, Kansas has been the focus of a number of previous studies into the use of MODIS time-series for crop classification (Wardlow and Egbert 2002, 2005; Wardlow, Egbert, and Kastens 2007; Wardlow and Egbert 2008), and has a very detailed and easily-accessible crop cover dataset in the form of the USDA CDL, making it a natural choice for a preliminary study area to test my method.

Table 3.1: Most extensive crops in Kansas, 2012
(adapted from US Department of Agriculture 2013).

	Acreage (1,000 acres)	Production (1,000 units)
Wheat	9,100	382,200
Corn	3,950	379,200
Soy	3,810	83,820
All Hay	2,750	4,340
All Forage	2,750	4,545
Sorghum	2,100	81,900

3.2   Pellegrini, Santiago del Estero, Argentina

Santiago del Estero, a province in Northwest Argentina, has an area of 136,351 square kilometers, about the same as Arkansas, but a population of about 874,000 (INDEC 2010b). The entire province is classified within the *Parque Chaqueño* (Chaco forest), but the forested area has declined rapidly in the past fifteen years. Over the period 1998 to 2002, 306,055 hectares were deforested (Secretaría de Ambiente y Desarrollo Sustentable [Argentina] 2007). From 2006 through 2011, a further 701,030 hectares of forest were lost, 283,669 of which were after the enacting of the OTBN (Secretería de Ambiente y Desarrollo Sustentable [Argentina] 2012). Over both of these time periods Santiago del Estero experienced the highest levels of deforestation in all of Argentina.

The Department of Pellegrini is an administrative area in the Northwest corner of Santiago del Estero (Fig. 1.1).[1] The department has an area of 6,944 square kilometers, a size slightly larger than the state of Delaware, and a 2010 population of only 20,514 (INDEC 2010a). The primary municipality of the department is Nueva Esperanza, with a population of about 4,500. The frontier nature of Pellegrini seems to have limited deforestation

in the department for some time, but the push for land has increased the rate of deforestation. Over the years 2001 to 2005, only 5,968 hectares were found to be deforested (Volante 2005). From 2006 to 2011 the area deforested increased to 75,349 hectares, some 39,480 hectares cut after the enacting of the OTBN, a rate much higher than previously witnessed (Secretería de Ambiente y Desarrollo Sustentable [Argentina] 2012). Of the area cleared post-OTBN, 2,181 hectares were in red areas, the highest clearing of that designation in the nation. The vast majority of clearing, however, was 29,796 hectares in yellow areas. While Pellegrini's total deforestation during the period 2006 to 2011 was not the highest in Santiago del Estero, as both Moreno Department and Alberdi Department had higher total deforestation, as a percent of total land area Pellegrini's deforestation occurred at a greater rate: 10.85 percent of Pellegrini's land area was cleared versus 10.45 percent and 7.91 percent of Moreno and Alberdi, respectively.

Volante et al. (2005) found Pellegrini's primary summer crop over the years 2000 to 2005 to be soy, averaging about 40,000 hectares cultivated per year. Corn was the second most frequent crop, occupying about 7,500 hectares per year. *Poroto*, a generic term for many types of common beans, were the third most popular, averaging a total cultivation of about 2,500 hectares per year. The primary winter crop was wheat, though cultivation varied wildly from less than 10,000 hectares in 2002 to over 31,000 hectares in 2004.

Chapter 4

Data and Methods

4.1   Overview

The purpose of this study is to develop a set of tools to allow the classification of agricultural crops using a time series of imagery and known crop reference signatures and test the portability of the reference signatures. The data used for this study consists of the following:

- 250-meter MODIS 16-day Composite Vegetation Index images

- 30-meter 2012 USDA Cropland Data Layer (CDL): agricultural land cover raster dataset

- 30-meter Landsat 8 Operational Land Imager satellite imagery

- Shapefile of the administrative boundary of the Department of Pellegrini

- 2014 Land cover vector dataset with crop identifications for Pellegrini

The first three datasets are publicly available from US agencies. The Pellegrini boundary is from the public Natural Earth Administrative Boundaries global dataset

CITE DATA SOURCE

. The land cover dataset for Pellegrini was digitized from Landsat 8 images (path 230, row 78), and the crop identifications were collected in the field.

An outline of the processing workflow is below:

1. Reproject the MODIS composite imagery

2. Assemble individual composite images into single time series images, one for Kansas and one for Argentina

3. Create a mask of all pure pixels (e.g. non-mixel) in the time series images

4. Use the CDL to isolate the pure corn, soy, and sorghum pixels in the Kansas time series image.

5. Identify the unique groups in each set of isolated pixels using k-means clustering

6. Extract the pixel values for each cluster from the time series image and find the mean value for each date to find the unique signatures for each crop

7. Validate the signatures by fitting the signatures to the time series image, then classifying the fit rasters to check the accuracy

8. Fit the signatures to the Argentina time series image

9. Classify the Argentina fit rasters and assess the accuracy

This chapter is a look at the theory and concepts behind this classification approach, the methods used to create the validation land cover dataset of Pellegrini, and the data processing steps used to generate the study results. Details about the specific tools in the classification toolset and the development process can be found in Appendix B. For a detailed explanation of all the testing proceeding this study, please see Appendix C. A thorough recounting of my field experience can be found in Appendix A.

4.2 Composite Vegetation Indices and Time-Series Images

The differentiation of crop types in remotely-sensed imagery is not a straightforward process. The use of a vegetation index (VI), such as the normalized difference vegetation index (NDVI) or the enhanced vegetation index (EVI), can help identify crops by their specific VI values in an image.

NDVI is a normalized ratio of the red and near-infrared bands, and can be expressed mathematically as:

$$NDVI = \frac{\rho_{NIR} - \rho_{red}}{\rho_{NIR} + \rho_{red}} \tag{4.1}$$

where ρ_{NIR} and ρ_{red} are the measured surface reflectance in their respective bands. As a ratio, the index minimizes multiplicative noise, but has issues with non-linearity and additive noise (Huete et al. 2002).

With advances in calibration, atmospheric correction, and other noise removal techniques, which are integrated into the MODIS data processing workflow, a ratioing index is less necessary. The EVI was specifically developed for the MODIS platform to help correct some of the deficiencies of the NDVI. It has better sensitivity to high biomass, canopy structure, and leaf area, and less susceptibility to atmospheric degradation. EVI is calculated as:

$$EVI = G\frac{\rho_{NIR} - \rho_{red}}{\rho_{NIR} + C_1 \times \rho_{red} - C_2 \times \rho_{blue} + L} \tag{4.2}$$

Again, each ρ is the measured surface reflectance in the respective band, after complete or partial atmospheric correction. The blue band is used to "subtract" aerosol effects from the red band. Additionally, four coefficients are introduced: G is the gain factor, C_1 and

C_2 are used in the aerosol calculation, while L "is the canopy background adjustment that addresses nonlinear, differential NIR and red radiant transfer through a canopy" (Huete et al. 2002: 196). The values of these coefficients as used in the MODIS EVI calculation are 2.5, 6.0, 7.5, and 1.0, respectively.

Some crops, such as soy and sugarcane, have very different spectral reflectance throughout their development and maturation, however others, such as soy and corn, can have very similar reflective curves, leading to overlapping VI ranges (Price 1994). Such overlap can make it impossible to determine a crop type with specificity using traditional approaches; even using hyperspectral data, few differentiating characteristics between crops can hinder classification. To combat this ambiguity, a time series of images can be used to find VI values throughout a year, allowing the development of a classifier based on annual phenology rather than a single-date image (Gu et al. 2010; Wardlow and Egbert 2002, 2005; Wardlow, Egbert, and Kastens 2007; Wardlow and Egbert 2008; Zhang et al. 2003).

MODIS 16-day VI composite imagery from both the Terra and Aqua Earth Observing System (EOS) satellites is available from the Land Processes Distributed Active Archive Center (LPDAAC).[1] Each MODIS satellite images the entire Earth daily: the Terra satellite makes its passes in the morning, while Aqua follows in the afternoon. This temporal resolution is the greatest advantage of the MODIS platform, as the likelihood of getting enough cloud-free data to develop a phenologic model is significantly increased over other common platforms like Landsat Thematic Mapper (TM) and Landsat Operational Land Imager (OLI), which only have repeat coverage every sixteen days. MODIS data, however, comes at the price of a reduced spatial resolution of 231 meters[2] compared to Landsat's 30-

meter pixels. At this resolution, crop mapping is restricted to medium farms and larger—those with fields of at least 250 meters square, though often a field must be up to two times larger in one dimension to ensure a pure pixel can be isolated. For the purposes of this investigation, however, this limitation is inconsequential, as small farms have a relatively minor impact on deforestation due to their size. Moreover, the crop of interest, GM soy, is only profitably grown using highly mechanized, input-intensive agricultural practices at very large scales. Small fields do not have high enough yields to overcome the significant capital investment required.

NEED A SOURCE FOR THIS—TALK TO POLO]

LPDAAC creates the VI composites using the maximum VI value over the proceeding 16-day time period. The images are numbered by the day of the year (DOY) of the last date in the image, so an image from DOY 17 is the composite of the images from January 2 through January 17.[3] Both NDVI and EVI are included in the MODIS VI products, and require no preprocessing for immediate use (unless cloud cover is pervasive in the area).

For this study, I chose to classify the 2012 Kansas summer growing season and the 2014 Argentina summer growing season. I assembled the MODIS 16-day composite VI images into multi-date time-series images (TSI) covering the growth cycle of the summer crops, where each band in a TSI is a 16-day composite VI, and the bands are ordered consecutively (see Appendix B.2 for the description of the Build Multidate Image Tools)

SHOW AN EARLY SEASON AND LATE SEASON VI SIDE-BY-SIDE TO ILLUSTRATE HOW VI VALUES DIFFER THROUGHOUT THE YEAR

. The Kansas summer TSI covered the date range DOY 97 through DOY 273, and

was made with data from the Terra satellite (LPDAAC product MOD13Q1, tile h10v05).

Prior to creating the TSIs, each of the 16-day composites was reprojected from the native

MODIS sinusodial reference system using LPDAAC's MODIS Reprojection Tool

CITE THIS TOOL

. I reprojected the Kansas data into the Albers Equal Area Conic projection for the con-

tiguous USA using the 1983 North American Datum (WKID: 5070) to match the reference

system of the USDA CDL.

In Argentina, as it is in the Southern Hemisphere and the seasons are inverted to those of

the Northern hemisphere, the growing season shifts, as must the date range for the VI time-

series. The TSI for Pellegrini must begin at the end of the proceeding year to adequately

capture the entirety of the summer phenologies. To accomplish this, the time-series image

for summer 2014 began with the 16-day composite image from DOY 345 of 2013 (or DOY

−20 with reference to 2014) and ended with the image from DOY 105 of 2014. This specific

date range was chosen based on information provided by local farmers to ensure coverage

of the earliest planting and latest harvesting dates, as well as manual inspection of pixel

signatures throughout the study area. Data through DOY 129 would have been preferred,

but persistent clouds prevented using that late-date composite and necessitated the switch

to the Aqua satellite's imagery (LPDAAC product MYD13Q1, tile h12v11). The Argentina

composite images were reprojected with the UTM Zone 20S reference system (WKID:

32720).

4.3   Crop Phenologies and Phenological Classification

Gu et al. outlined that phenological statistics regarding vegetation development can be derived from a MODIS VI time-series, including "start-of-season time (SOST), start-of-season NDVI (SOSN), end-of-season time (EOST), end-of-season NDVI (EOSN), maximum NDVI (MAXN), maximum NDVI time (MAXT), duration of season (DUR), amplitude of NDVI (AMP), and seasonal time integrated NDVI (TIN)" (2010: 529). A principal component analysis (PCA) can then be used to extract the meaningful variation in the data. Similarly, Wardlow, Egbert, et al. (Wardlow and Egbert 2002, 2005; Wardlow, Egbert, and Kastens 2007; Wardlow and Egbert 2008) showed that a decision tree classifier can be used to classify vegetation time-series data into increasingly refined categories until specific crop types are isolated and classified. By beginning with a basic land cover classification (e.g. forest, urban, agriculture), crops in the agriculture class can be broken down into winter and summer varieties using peaks in the vegetation index (winter wheat will peak earlier in the year than summer crops like corn and soy). Then, using training sites of known crop types defined by ground truth data, a final crop classification can be assigned by finding pixel values for key dates where like crops can be differentiated. That is, using the growing season in the Northern Hemisphere as an example, if from the training sites we know crop A has VI values between 0.7 and 0.8 on June 26 and between 0.5 and 0.6 on August 29, while crop B is between 0.55 and 0.65 and 0.75 and 0.85 on the same dates, pixels in the summer crop class can be assigned one of these types by testing their pixel values on these dates. While the authors found this method to have about an 85 percent overall accuracy

(Wardlow and Egbert 2005), the downside of this method is that it requires training sites with previously-determined crop types to produce a classification, which can be time consuming and expensive to acquire.

Masialeti, Egbert, and Wardlow (2010) found that VI values from one year have a significant correlation with values from other years. Comparing the phenological curves of crops formed by the NDVI values from 2001 MODIS data (from Wardlow and Egbert 2005) with those from 2005 MODIS data, the authors found the overall shape of each crop's curve is maintained year-to-year, with a subtle shift in the beginning of the curve (earlier or later planting), a scaling of the maximum of the curve, and and scaling of the spread of the curve (a longer or shorter growing season), depending on weather and other external variables (Fig. 4.1). They surmised, with a means to account for the shift and scaling of the curve, one could use VI values from one year to classify those from another.

Even without a mechanism to account for interannual differences, Brown et al. (2007) used crop phenologies derived from multiple years of data to test four phenological classification methods. The authors fit the known phenologies to the unknown phenologies from other years by comparing the VI values throughout the growing season. The degree of likeness between a known VI curve and the unknown VI curve determined the classification. They showed that the best of the four classification methods was to find the sum of the square errors between the known and unknown curves (the SSE method, pg. 131).

The similarities between the methods presented in Brown et al. and hyperspectral remote sensing techniques are striking. Hyperspectral techniques compare known spectral *signatures* from a signature library to the unknown pixel signatures in an image. One method,

Figure 4.1: Examples of transformations of a crop's VI curve due to interannual

variations in growing conditions. The original curve was derived from soy in southwestern

Kansas. The other curves were arbitrarily adjusted to illustrate each of the possible

transformations.

spectral feature fitting, uses a least-squares comparison reminiscent of SSE fromBrown et al.
(Exelis Visual Information Solutions 2013; Clark et al. 2003). The key difference between
the two, besides comparing reflectance across time versus reflectance across the electromag-
netic spectrum, is that spectral feature fitting does not require any training data from the
processed image. All of the spectral signatures used for identification are from standardized
spectral libraries, containing many spectra of different materials.

Accordingly, one goal of this study is to realize a method of vegetation classification us-
ing multi- or hyper-temporal imagery that does not require training data to be extracted
from the imagery itself, rather relying on standard libraries of *temporal* signatures for differ-
ent vegetation and non-vegetation land covers. A major challenge of this idea is that, unlike
spectral signatures, temporal signatures are not necessarily consistent location to location,
nor year to year as mentioned above. A viable classification method thusly must provide
a way to transform the temporal signatures, within appropriate bounds, to match the hor-
izontal scaling, vertical scaling, and time shifting of an unknown pixel before finding the
degree of fit between the signature curve and the pixel curve.

Sakamoto et al. (2005, 2010) demonstrates a method using MODIS time-series data for
use in finding key dates in a crop's phenology, enabling better crop management strategies.
Specifically, the authors' two-step filter (TSF) method uses a wavelet transformation and a
constrained minimization function to find a reference signature for a specific crop's pheno-
logical development, and then fits that signature to known pixels of that crop type, finding
the scaled dates of key transitions between developmental stages in the plants' growth. This
TSF method demonstrates that reference signatures can be fit to a pixel's signature using a

minimization function, accounting for the variations from the reference curve and the pixel curve. This minimization method provides the means to account for the scaling and time shift differences, allowing previously-known temporal signatures (e.g. not from training sites) to be fit to pixel signatures in a VI TSI.

Specifically, from page 2151 of Sakamoto et al. (2010):

$$RMSE = \left[\frac{1}{365/s} \sum_{x=j(0),j(1)...}^{n} \left(f\left(x\right) - g\left(x\right) \right)^2 \right]^{\frac{1}{2}} \tag{4.3}$$

where n is the number of dates in the TSI, $f(x)$ is the phenological curve for a given pixel in a dataset, and x is the DOY, as defined by $j(y)$:

$$j\left(y\right) = k\left(i \cdot s\left(y - 1 \right) \right) \tag{4.4a}$$

$$\text{where} \quad k\left(z \right) = \begin{cases} z, & \text{if } z \leq 0 \\ \\ (z \bmod 365) \bmod i - 1, & \text{if } z > 0 \end{cases} \tag{4.4b}$$

such that s is the interval of the imagery and d is the starting date of the imagery. $g(x)$ in Equation 4.3 is given by:

$$g(x) = yscale \times h\left(xscale \times (x + tshift)\right) \tag{4.5}$$

Here, x again is the DOY, $yscale$ and $xscale$ are coefficients controlling the vertical and horizontal scaling of a reference signature $h(x)$, and $tshift$ is a constant representing the horizontal shift, in days, of $h(x)$ (see Fig. 4.1). Thus, if we minimize Equation 4.3 bounding $yscale$, $xscale$, and $tshift$ in $g(x)$ with reasonable values for each, we can calculate how well a given reference temporal signature $h(x)$ can be made to fit the pixel signature $f(x)$. Comparing a pixel's RMSE fit value from each of the reference signatures allows final

classification; the signature with the lowest RMSE value has the best fit, and, of the tested signatures, provides the most probable identification.

4.4   Field Methods and Data Collection in Pellegrini

While ground truth data was easily available for the Kansas study site, getting a ground truth dataset for verification of the classification in Pellegrini was not so simple. Such a dataset did not exist, necessitating onsite data collection. I visited Argentina mid-March to early April 2014 to gather field observations of summer crop types and to talk to local farmers about typical agricultural practices, summer and winter crop varieties, and planting and harvesting dates.

To guide my ground truth collection, I generated 400 random points inside the Pellegrini shapefile boundary, and used a Landsat OLI image as a reference for land cover (image date February 5, 2014). Where a point fell within a mixel, I allowed it to be moved within a 3-by-3 pixel window centered on the point's original pixel, trying as much as possible to keep the point within a pixel belonging to the feature type on which it originally fell. In certain limited cases, if a point fell quite obviously within a field but the center pixel and eight surrounding pixels were mixels and/or were not within the field, I allowed the point to be moved to the closest full pixel of the same continuous field. Of the 400 points, I had move 106 within the 3-by-3 window, and ten to a non-neighboring pixel within the same field.

The primary means of gathering the crop identities to complete the ground truth was direct observation. However, this strategy proved to be difficult in many cases; often, fields

were not accessible due to road conditions or locked gated. Data not from direct observations came from interviews with farmers and land owners. In such cases, the interviewees were asked to identify their fields on printed maps with the reference Landsat imagery and describe their cultivars. The data from observations and interviews was recorded directly on the maps and later manually digitized.

Ancillary information about agricultural practices in the region was also collected whenever possible. It was a key goal to identify each crop's date range for planting and harvesting in order to allow the proper selection of MODIS imagery dates and setting of the $tshift$ bounds for Equation 4.5.

4.5   Data Processing

4.5.1   Resampling the CDL

To use the CDL as a ground truth with the Kansas TSI, the 30-meter CDL pixels were resampled by majority to match the larger TSI pixels. This allowed a direct comparison between the crop values from the CDL and the pixel signatures in the TSI.

4.5.2   Eliminating Mixels

After building the TSIs, the next processing step was to eliminate mixels from the TSIs, to prevent errors caused by mixed temporal signatures (see Appendix C.2 for more information). Pure pixels, the non-mixels in the image, were isolated by intersecting the ground truth datasets with a vector grid of the TSI pixels. All pixels with an area greater than a

certain area threshold were then selected as pure. I also manually selected two sorghum pixel features that were omitted due to intermixed soy pixels. I chose to add these pixels due to the low number of sorghum features retained, and that the intermixed soy appeared to be errors. Only these pure pixels were classified; the mixels in the images were ignored.

The original 30-meter CDL raster served as the reference for finding the pure pixels in the Kansas study site. The raster was converted to vector polygons and intersected with the TSI grid polygons. From the resulting geometry, all polygons greater than 53,000 square meters (or 98 percent of a full MODIS pixel) were selected as pure.

For the Argentina analysis, the digitized features of identified fields were combined with manually digitized features of all large forested areas, unknown fields, and "other" areas. Some places where the land cover was mixed and could not be visually differentiated were not digitized and were considered to be composed entirely of mixels. The complete dataset of land cover was then intersected with the Argentina TSI grid. Through trial and error, a minimum area of 50,000 square meters was used to select the pure pixels in the image.

4.5.3   Extracting the Reference Temporal Signatures

As a reference library of temporal signatures does not yet exist, I had to extract my own signatures from the Kansas TSI. To do so, the pure TSI pixels of each key summer crop— corn, soy, and sorghum—as specified in the resampled CDL were isolated in separate rasters. Each of separated rasters was clustered into three clusters using the ENVI

Cite ENVI

k-means tool with a 1.0 percent change threshold over 100 maximum iterations. The

TSI pixels in each cluster were then sampled and averaged to find the three primary signatures for each crop[4] see Appendix B.3 for information about the Extract Signatures Tool).

4.5.4   Fitting the Reference Signatures to the TSIs

Equation 4.3 was implemented in Python with a command line interface to allow easy processing of the TSIs. Details of the tool can be found in Appendix B.4. The tool iterates through every pixel in a TSI, comparing each reference signature with the pixel signature. The tool is able clip an input TSI to either pixel bounds or a shapefile containing a polygon, and can also use an optional point shapefile to limit the processed pixels to only those coincident with points. An output raster is created for each signature to record the RMSE from every pixel comparison.

The reference signatures extracted from the Kansas TSI clusters were fit to the TSI to verify the classifier. The TSI was clipped Then, the same Kansas signatures were fit to the Pellegrini TSI. The fit rasters from each TSI were then classified. In both cases, the bounds for the $xscale$ and $yscale$ parameters were 0.6 to 1.4. The $tshift$ bounds for the Kansas processing were -10 to +10 days, while the bounds for the Pellegrini processing were 120 to 140 days (still ± 10 days, but shifted 130 days).[5]

4.5.5   Classifying the Fit Rasters

The classification process is complex; Appendix B.5 contains a full discussion of the process, so I will refrain from a lengthy description here.

Classifying the fit rasters first requires thresholding the values in each raster, then finding

the lowest value for each pixel. The signature with the lowest thresholded fit value has the best fit, and the pixel is classified as that crop. The thresholding prevents pixels with poor fit values from being classified as a crop. If a pixel has no remaining fit values after thresholding, it is classified as "other." Currently, appropriate threshold values are not well understood, so to find the best classification, the classification tool must brute-force through many combinations of thresholds within a user-specified range, classifying the fit rasters, and calculating the accuracy of each threshold combination in comparison with the ground truth dataset. A raster of the classification with the best accuracy is retained.

Chapter 5

Results

5.1 Ground Truth for Pellegrini

The digitized polygons for both identified and unknown features are shown in Figure **??**.
The area of each of the land cover classes is broken down in Table 5.1.

Of my 400 sample points, I was able to visually classify 247 of the points as forested
from Landsat OLI imagery before leaving for Argentina. Of the remaining 153, I identified
102 as actively-cultivated agriculture: thirty five points as corn, twenty three points as soy,
two points as sorghum, five points as poroto, and thirty seven points as pasture. Twenty
one points were identified as "other," representing all non-forest, non-agricultural, and/or
mixed-use land cover classes. Another three points, based on the literal description com-
municated to me by the land managers, were identified as "nothing." I am unsure if these
fields were simply left fallow or are something else, but they are not under active cultivation.
Twenty seven points could not be verified due to inaccessibility or falling on a mixed-use
area, and were removed from the final set of sample points used for the accuracy assessment.

Table 5.1: Summer 2014 Pellegrini Land Cover Classes
By Area, with Sample Point Counts

Cover Type	Hectares	Sample Points
Forested	389,541	247
Other	41,588	21
Corn	40,818	35
Pasture	35,057	37
Soy	27,240	23
Poroto	9,539	5
Nothing	3,057	3
Sorghum	1,646	2
Unknown	93,808	21
Omitted	52,051	6
Total	694,346	400

5.2   Elimination of Mixels

I found 1,359 pure pixels in the 100 pixel by 100 pixel Kansas study area. Clipped to boundary shapefile, the Pellegrini TSI contained 129,873 pixels total, of which 97,054 were pure. The numbers of pure pixels in each of the summer crops of interest are shown in Table 5.2. It is interesting, though perhaps nothing more than a curious coincidence, that the percent of the total pixel count for each of the crops is roughly equal between the Kansas study site and Pellegrini, omitting the unknown fields. However, the lower level of overall development in Pellegrini is reflected by the tenfold increase in pure pixels of all other land covers, primarily due to the high amount of forested area.

FIGURE OUT HOW TO USE S COLUMN FROM SIUNITX TO ALIGN NUMBERS ON DECIMAL POINT WHILE USING CENTERING FOR COLUMNS

Table 5.2: Mixel and Pure Pixel Counts

	Summer 2012 Kansas TSI		Summer 2014 Pellegrini TSI	
	Count	Percent of Total	Count	Percent of Total
Total Pixels	10,000	100.00	129,873	100.00
– Pure Pixels	1,359	13.59	97,054	74.73
– Corn	414	4.14	5,855	4.51
– Soy	354	3.54	3,936	3.03
– Sorghum	16	0.16	183	0.14
– Unknown	n/a	n/a	10,676	8.22
– All Others	575	5.75	76,404	58.83
– Mixels	8,641	86.41	32,819	25.27

5.3   Extracted Reference Signatures

Before extracting the reference signatures for each summer crop, the pixels for each crop

had to be clustered. Figure

INSERT REFERENCE TO MAP HERE

shows the spatial distribution of the three clusters for each crop. Given the small number

of pixels, the k-means algorithm only found a single cluster for sorghum.

The temporal signatures of each of the clusters are plotted in Figures

INSERT REF TO FIRST FIGURE

through

INSERT REF TO LAST FIGURE

. Each of the crops have a somewhat similar appearance to one another, but each can

be differentiated: corn peaks earlier in the year than soy or sorghum, soy has the highest

peak VI value of the three, while sorghum has much lower VI values than soy and a slightly

longer growing season.

FIGURE 4-UP OF MAPS OF CLUSTERS KS

SIGNATURE PLOTS OF EACH SUMMER CROP
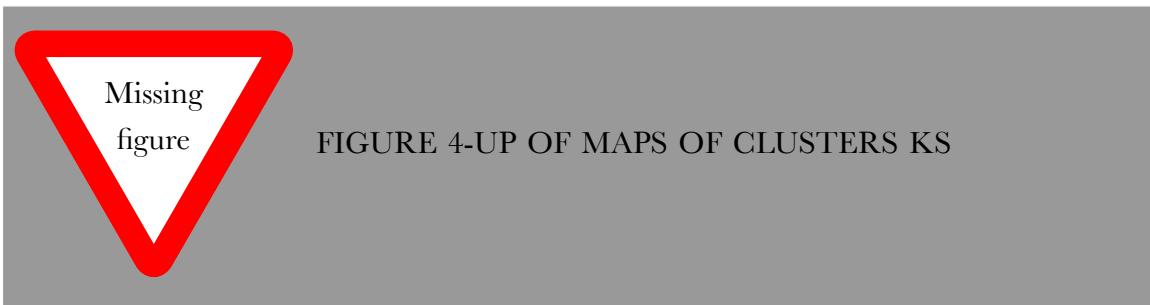
5.4   Fitting and Classifying the TSIs

Fitting the seven crop reference signatures—three corn, three soy, and one sorghum—to the TSIs produced seven fit rasters for each TSI. The minimum values were typically in the range of 175 to 250, while the maximum fit values were often around 3000.[1]

The Kansas classification achieved an accuracy of 84 percent, a map of which is shown in Figure

Insert ref to map

; the confusion matrix is Table 5.3. This classification was generated by iterating over the range of thresholds from 400 to 1150 by steps of 150. The best threshold combination from that process was then manually adjusted by steps of 50 for each fit raster until the

Table 5.3: Summer 2012 Kansas Study Site Classification Accuracy

		Reference Data					
		Corn	Soy	Sorghum	Other	Total	User Acc.
Classified	Corn	369	65	5	18	457	80.74%
	Soy	32	273	11	48	364	75.00%
	Sorghum	0	0	1	4	5	20.00%
	Other	13	16	1	503	533	94.37%
	Total	414	354	18	573	1359	
	Producer Acc.	89.13%	77.12%	5.56%	87.78%		

Overall Acc.: 84.33%

Kappa: 0.76

Table 5.4: Kansas Best Classification Thresholds

Signature	Threshold Value
Corn 1	1000
Corn 2	750
Corn 3	500
Soy 1	750
Soy 2	1300
Soy 3	500
Sorghum	400

maximum accuracy classification was found using the thresholds in Table 5.4.

The Argentina classification was not nearly as successful. While the best accuracy was also 84 percent, it occurred at a threshold value of 1 for all seven fit raster, essentially classifying the entire study area as "other." The resultant accuracy was simply due to the high number of sample points that were not the three crops of interest (see Table 5.5.

Confusion matrix for 500 all thresh

Table 5.5: Summer 2014 Pellegrini Best Classification Accuracy:
Threshold of 1 for Each Fit Raster

		Reference Data					
		Corn	Soy	Sorghum	Other	Total	User Acc.
Classified	Corn	0	0	0	0	0	0.00%
	Soy	0	0	0	0	0	0.00%
	Sorghum	0	0	0	0	0	0.00%
	Other	35	23	2	315	375	84.00%
	Total	35	23	2	315	375	
	Producer Acc.	0%	0%	0%	100.00%		

Overall Acc.: 84.00%

Kappa: 0.00

Chapter 6

Discussion

- Signatures found by kmeans in KS are not wildly variable - Perhaps separates pixels that would be considered quite similar using the fitting algorithm - Maybe this means the clustering should be based on the fit of each pixel to one another; pixels with low fit values to one another would be grouped together

   - Notice how the KS clusters roughly delineate fields - Shows that each pixel in a field of multiple pixels typically has a very similar signature to all the others in the field - Makes sense as the crops in each pixel grew under the same conditions, so should have the same development

Appendix A

The Story of My Field Work

In order to complete an accuracy assessment of the classification I was to produce of agriculture in Pellegrini, I knew I needed ground truth data with which I could compare my results. As I suspected would be the case, I was unable to find any extant datasets, so I knew I would have to visit Pellegrini to gather such data.

After extensively reviewing satellite imagery of the area, I knew the fields were very large and appeared to have many roads connecting them, so I did not expect access to be problematic. While the size of the department, 6,943 square kilometers, is about the size of Delaware, I thought I would be able to cover ground fairly quickly, and allocated three weeks of time in Pellegrini to gather all my data.

I did have concerns to how the local people would take to my project. I know that I would be immediately suspicious of some foreigner coming in to my town and wanting to know everything about the agricultural practices in the area, including visiting all of the fields. I actually practiced how to say, in Spanish, "Don't shoot! I am leaving, there is no problem." Perhaps this is just an American thing, but I was expecting, at some point, to be

confronted by someone with a gun who did not like me. After all, I am not necessarily in favor of the agriculture that is taking over the area, and while I tried to present my views as neutrally as possible, I thought a conflict would be inevitable.

I arranged for a small rental car in San Miguel de Tucumán, Tucumán, a city about 150 kilometers from Nueva Esparanza. I knew the roads would not be great, but I figured I should be able to get through just about anything with the rental car, except mud. Nueva Esparanza was to be my base, and my plan was to try and visit the furthest areas first, as I expected those to the most difficult to access, leaving the easier areas for last.

As mentioned in my methods, I randomly generated 400 points throughout the department to survey. Of those 400, I immediately identified 247 of them as forested using Landsat imagery, which meant I did not need to visit them. For the remaining 153 I did need to visit, I created map sheets—one for every point, centered on the point—showing the point at three different scales: an overview at 1:60,000 scale, a closer image at 1:30,000 scale with the MODIS pixel grid overlaid, and a very large scale 1:4,500 scale view with older but higher resolution imagery from Digital Globe. I also created a 25-kilometer grid over Pellegrini, which I used to make eighteen smaller-scale "regional" maps at 1:150,000 scale to help identify neighboring points and plan routes. Lastly, I made an overview map of the entire department at 1:475,000 scale. I printed all of these maps and put them in a binder[1]. I planned to collect data about as many fields as I could, even those without sample points, and I got metallic markers so I could outline each field on the maps and take notes of crop types.

Getting to Nueva Esparanza was a challenge in itself. Due to the budget fare the airline

provided me in exchange for my miles, it took me some 36 hours just to get to the hostel in Buenos Aires. Once there, I had to make my way around town to gather some supplies and change money. I had a short night in the hostel, as I needed to make an early flight from Buenos Aires to San Miguel de Tucumán. I picked up my rental car at the airport in Tucumán, at which point my stress level increased significantly, as I now had to make my way around the city not as a passenger, but as a driver. Argentine traffic laws do exist, but my perception is that, generally speaking, no one knows what they are.

Another problem was gas. Even something as simple as purchasing fuel for one's vehicle can become a new and stressful experience in a foreign country. After visiting Guatemala, where drivers would pull up to random buildings around town and attendants would appear from nowhere with a container of gasoline and a makeshift funnel made from the top of a plastic bottle, I was unsure what to expect. It turned out that the process was not so rudimentary nor much different from buying fuel back home, and my concern was mostly unwarranted.

After driving throughout the city gathering supplies, it was time for me to head to Nueva Esparanza. Despite using two maps and my GPS to try and navigate my way to the correct highway, I found myself on the wrong road out of town, and had to spend an inordinate amount of time following a long string of slow moving cars along what seemed more to be a series of main streets through a corridor of small towns than a highway. Thankfully, however, the road eventually led to the route I initially intended to take, and I began to make more rapid progress towards Nueva Esparanza. Unfortunately, my rapid progress quickly slowed upon reaching the beginning of road construction, which persisted the next 70 km

or so.

My first full day I was in Nueva Esparanza I planned out a long route to investigate, but, after talking with some of the workers of the hotel I was staying in about my security concerns, I decided I should visit the police *comisaria* to ask if I was going to have any problems with land owners or locals while working. The first moment I opened my mouth I became the attention of everyone in building. I used the best Spanish I could muster to try to tell them what I was there to do and why, but I kept getting passed from person to person. Eventually, based on the questions they were asking me—things I was sure I had already said—I realized they could not understand me. And I was struggling mightily myself to understand them.

After what must have been two and a half hours and close to forty people interviewing me,[2] they were finally able to track down an English teacher who taught in the local schools. With his assistance, I was finally able to communicate the details of my project, and they were able to provide me with an official document vouching for my identity and purpose in case anyone took issue with my presence. They assured me that I would not have any problems with the people. Not once during my trip did I need the document.

In spite of the late hour I left the police station that first day, I naively decided to attempt to complete the long route I had laid out for myself. My early progress was actually quite good; I did not check off many points, but I was able to visit quite a number of fields in a short amount of time. This only served to errantly bolster my self-confidence.

In line with my plan to visit the furthest points first, I was making my way to the far northwest corner of Pellegrini. About an hour and a half from Nueva Esparanza, I came to

the border with the province of Salta. Looking at the Landsat imagery, I could clearly make out a long, straight road following this line. That this road was not marked on any other maps should have been a clue to me.

After a few minutes of searching and considering the numerous side paths along the main road, I determined the correct road to follow, and proceeded to head north along it. I had a thought about the sandiness of the road, but knew that as long as I maintained my momentum I should not have any problems. I did not consider the hour, which was closing in on 5:00 PM, nor the fact that, due to my lengthly visit with the police, I had not taken the time to eat that day, aside from a breakfast consisting only of a banana.

Only a few minutes down the road, the situation quickly worsened. Deep ruts suddenly appeared in the middle of the road, and I did my best to straddle the car over the left one by attempting to drive with my left tires on the side of the road and my right tires down the middle. However, the success of this maneuver was short lived, and before I knew it, the small, low car had dropped down into the ruts. I stepped on the gas, hoping that keeping the car moving would keep me for getting stuck. The sound of the sand scraping at the underside of the car was unbearable. I spotted a break in the vegetation on the left side of the road, so I pointed the car at it, hoping the wheels would be able to break free from the ruts with a sharp enough turn. Luckily, this time my maneuvering was successful, and I found myself parked on the only hard patch of clear ground in visible surroundings.

I got out of the car and surveyed the situation. The deep, sandy ruts continued in both directions along the road. Being only a few minutes from the main road, and realizing the lateness of the hour, I figured the only reasonable course of action would be to return to

Nueva Esparanza. I contemplated driving through the small brush along the side of the road to get back to where the ruts were shallower, but I figured my tires would have been no match to the large thorns common to so many of the Chaco's plants. My only regress would be to attempt to drive back the way I came.

Careful of the thorniest of plants, I managed to turn my car around, orienting it in the proper direction. I knew I needed to do two things if I were to make it back to the main road without problems: go fast, and stay out of the ruts. I was able to do neither.

I stepped on the gas, but given the gearing of the Chevy and its abysmally-small power plant, quick of the line it was not. Adding to the fact that I was wholly unsuccessful at keeping out of the ruts, I managed all of three or four meters before losing all forward momentum. I tried rocking the car by repeatedly shifting between first and reverse, but only managed to get the car more firmly planted in the sand.

Thanks to the sound advice of Polo, one of my committee members, I had actually purchased a shovel the day before in Tucumán. To say that at this point the shove came in handy would be an understatement.

I proceeded to dig out all the sand underneath the car upon which it was high centered, as well as a short path both in front and behind the car, and attempted another run at freedom. I repeated these steps numerous times with no success. Each time I felt that much closer to collapse due my plummeting blood sugar.

Some time into this cycle a woman approached on a motorcycle with her two kids. I stood there, staring at her as she drew closer, hoping she would stop and tell me she would be right back with someone to help me out. Instead, she stopped and began looking at me

as if amused as I proceeded to explain my predicament as best I could. She told me in the most unhopeful manner that she would send someone my way, if she found anyone who could help. I still wonder what became of that woman and her two kids.

Eventually, I became wise to my insanity, and decided I needed to try another course of action. I recognized my problem was acceleration: each time I tried to accelerate, my tires would dig into the sand, and the ruts would present themselves as that much deeper. In order to escape the situation, I needed to be able to get my car to speed before I encountered any ruts.

I quickly went to work regrading a 30 meter length of road. By this point I was on the verge of passing out, but I knew I could not take a break. Even if it had dawned on me that I could have eaten one of my cup of noodles raw (the only food I had in the car due to a misjudgment in preparation for this day trip) I could not have stopped to do so, as I needed to get myself out before dark or I would be stuck there all night.

After what I estimate to be two hours of hard work in that energy-sucking heat, I finally managed to clear what I hoped would be a long enough section of road to get me free. Getting back into my car, I resigned myself to spending the night out there, my cynicism taking hold and condemning me an attitude of hopelessness. Yet, in spite of my natural inclination for pessimism, I found my car floating over the sand, making its way toward freedom. I did not let of the accelerator until I was sure I was free of the clutches of the sand, which, looking back, actually may not have been until I was safely parked outside my hotel.

At this point I knew my whole plan was falling apart. I had planned to visit some twenty-

five points that afternoon, yet I only made it to four. I thought I could depend on myself to get around, but I realized my car was woefully incapable of passing all but the most traveled of roads. Moreover, many of the "roads" I had spotted on the satellite imagery and was depending on to get to my points were not in fact roads, but private paths behind fences, gates, and rows of bushes, accessible only to those with the permission of the landowner.

Even the roads that were accessible were beyond my worst nightmare. Perhaps my definition of bad was inaccurate; even when people told me before my trip the roads would be bad, I just said I'd be fine. I've driven on bad roads; what could be the problem? This is not to say I did not expect to have *any* problems with the roads, but to see the condition of the main roads—all potholed, rutted, sandy, and muddy—and to get stuck on my first day out, was a humbling and troubling experience.

I needed help.

The road conditions were not the only reason either. My interactions with the police officers at the comisaría should have been a clue to the difficulty I would have communicating. Argentine Spanish is particularly difficult on its own (if one has learned Mexican and Central American Spanish as I have), but the Spanish in Pellegrini is another dialect entirely. Take Argentine Spanish and add indigenous terms and the accent and idioms of an isolated rural area, and I felt like I was trying to learn another whole language. If I could have chosen one thing to have made my trip smoother, it would have been a better command of Pellegrini Spanish. I was able to get by, and came to understand some individuals fairly well, but often I found myself unable to communicate effectively.

I became clear to me that I needed to break out of my comfort zone and rely on others.

Doing so was very hard for me, as I tend to be extremely independent and like to do everything myself. I set unreasonably high standards, and few, including myself, can live up to them. However, I was clearly not succeeding on my own; I needed people that could get me to the places I had to see. It turned out that the English teach just so happened to have a motorcycle, and graciously agreed to take me out to survey points in the afternoons when he had free time. He also introduced me to a local teenager, who, despite his age, proved to be a worthy guide, as he knew the area and some English. His grandfather also had a truck, which helped us get around.

In working with these guides, I quickly came to learn that I was going to have the best success not in going to every survey point myself, but in talking with local farm hands and landowners. Even with the right vehicle, many places were still inaccessible, primarily because many "roads" on the satellite imagery didn't connect, or were blocked by locked gates. Luckily, I was introduced to one police officer in particular whose main function was to know everything and everyone in Pellegrini. Not only did he know what roads I could and couldn't drive on in my car, but he also had a way with people that allowed him to get much more information that anyone else I worked with. By far, the connections I made through him and the subsequent interviews supplied the majority of the data I collected. One such connection was with his cousin. His cousin was not only exceptionally knowledgable about agriculture in Pellegrini and managed quite a number of fields, but actually took it upon himself to gather some of my data for me, visiting some rather remote fields and talking with a number of other producers he knew.

Trusting people—especially people I do not know—with a project as big and important

as my master's thesis took an intentional act of letting go. I had to realize I needed skills and knowledge I did not have, but those around me did. This was doubly hard considering my inadequate lingual skills, and that at times communication would break down. What's more, I couldn't decide who was going to help me; the people I preferred to work with were not always available, so I had to turn to others I would not necessarily have chosen. Anyone doing fieldwork must be prepared for this reality: you can't choose the people that will be willing to help you.

I suppose I already knew I would need to do this, intellectually, but actually being able to was a learning opportunity for me. Letting go and trusting did not come easy, and often didn't really happen; I merely internalized my uncertainty in others as stress.[3] Yet, despite the overwhelming stress I inflicted on myself during some particularly "trusting" moments, *nothing bad happened*. I got my data. I was never robbed. I was never left stranded in the middle of nowhere (except of my own doing). My car got repaired and I didn't get ripped off. I survived.

Another realization: you never know what someone might be able to offer you. That is, I found it important to talk with everyone around me. Sometimes is was merely a different perspective or insight, while other times it was information which enabled me to cross of a couple points, but I realized everyone had something to tell me. I am an introvert and not outgoing, so I tend to shy away from most people, yet I was forced to interact with everyone. Many people I honestly would have avoided under different circumstances. I even found myself doing things that made me uncomfortable just to build my credibility, such as going to the *boliche* at three in the morning and trying (and failing) to dance to the popular music.

Surprisingly, I ran into a couple landowners in the club that night, and I could tell their impression of me was positively affected just by me being there. Joining in the cultural customs builds a rapport better than anything else.

These activities and having to build relationships I would normally have avoided pushed me outside my comfort zone and were a great opportunity for personal growth. Reflecting back on the trip and my life since returning, I can see a greater degree of social confidence. I am still shy and introverted, but I no longer feel unable to put myself out there when meeting new people. Moreover, some relationships I might have otherwise written off turned into good friendships.

As is evident, I was overly confident in my abilities, and consequently made a number of incorrect assumptions about how my work would go. Thankfully, of all things, the data collection maps I made worked very well. If I were to have to plan such a project again, I would struggle to identify any changes I would make to them. I will say that I overestimated the usefulness of the maps for navigation; my GPS receiver with a satellite image and my sample points loaded onto it proved to work much better, as I never had to find my location on the map before identifying the next turn. The obviousness of this strikes me now; I am just grateful that I was able to download the necessary software, despite my phone's seemingly nonexistent data connection, to make such a solution possible. Next time I will be sure to have my GPS setup beforehand.

And, to reiterate: one must trust in others. They will help. I expected them to not. Perhaps that is because their culture is more relational, or perhaps I am simply too untrusting. In any case, it is foolish to think that one can go into another culture without the expert

knowledge the locals have of the place and customs[4] and be able gather any data, whether those data are of the physical geography, of technical practices, of cultural customs, or of anything else. I had to rely on wonderfully helpful people to do that actual data collection; I was merely along for the ride, perhaps directing, but still little more than an observer.

Appendix B

Developing the Processing Tools

Development has been a very iterative process, and has been primarily driven by testing requirements (see Appendix C). Many of the core functions began as simple proof-of-concepts. As the codebase grew, it underwent significant refactoring. As this is my first major development project, I had to learn—the hard way—how to properly structure a project of this nature. I arrived at many key design principles quite late; some pieces of the project, consequently, were rewritten multiple times. Simultaneously, testing necessitated better ease of use and increased functionality; many features, such as the command line interface to the tools, were added as the need arose and better code organization made implementation possible. With the code as it currently stands, I believe my tools are just as easy to use as GDAL[1].

B.1 Review of the classification process

To reiterate, classifying imagery is a multi-step process. To do so is roughly as follows:

1. Build a multi-date image stack or time series image (TSI) from single-date images.

2. Find "pure" or mostly "pure" TSI pixels (eliminate mixels).

3. Obtain a reference temporal signature for each of the crops to be identified in TSI.

4. Run the fit algorithm using the phenological reference curves to generate the fit rasters for each of the input reference curves.

5. Use the threshold tool to find the optimal threshold settings for each of the fit rasters (requires ground truth data for accuracy assessment). This process should output a final classified image.

Steps 1, 3, 4, and 5 have been abstracted into individual command line tools, each of which is detailed below. Step 2 is currently a manual process, the procedure for which is detailed in section [TODO: LINK TO METHODS SECTION DISCUSSION ON MIXELS]; how this step was established is explained in Appendix C.2. A few other command line tools, such as to plot signatures or to create masked rasters, were also developed, but are not described here. See the project source and documentation on the github site: https://jkeifer.github.io/pyhytemporal. [TODO: VERIFY THIS IS THE CORRECT ADDRESS; SHOULD THIS BE INCLUDED? I HAVE NOT YET BEGUN WRITING THE DOCUMENTATION, AND WHILE I'D LIKE TO, IT IS POSSIBLE THAT IT WILL NOT HAPPEN]

B.2   Creating Time Series Images

Before I could complete any testing, I had to first determine a way to create a chronological multi-date image stack—a time series image (TSI)—in which the values of each pixel represent the temporal signature of its contents. A TSI can be thought of as the temporal equivalent of a hyperspectral data cube, and is the primary data structure used in the analysis.

Despite the fancy terminology, however, a TSI (or hyperspectral data cube, for that matter) is merely a multi-band raster file, where each band is the data for a given date (or for a spectral band, in a data cube). Abstracting this concept a step further, a raster file is simply an array. A single-band raster is therefore a two-dimensional array where the columns and rows of the image are represented by the columns and rows of the array, and the data are single-dimension values in each cell. Adding multiple bands, or in this case dates, to the image is easily accomplished by adding another dimension to the array.

The Python Geographic Data Abstraction Library (GDAL) and numpy libraries include objects and methods which make opening spatially-enabled raster files as arrays, saving arrays to spatially-enabled raster files, and manipulating arrays in memory trivial tasks. Thus, creating a tool to build a TSI from a selection of single-date raster files was straightforward and easy, and did not require any extensive or involved testing.

The finished tool, which I call the Build Multidate Image tool, simply requires the user to specify a director containing the MODIS .hdf files that will be assembled into a TSI. The the name of the VI the tool should extract from the .hdf files is an optional argument, as the

tool defaults to extracting the NDVI raster data.

B.3   Extracting Reference Temporal Signatures

While I hope in the future libraries of temporal signatures will allow researchers to use temporal classification tools without needing to derive their own signatures, obviously such resources are not available now. For my work this necessitated that I devise a tool to create such signatures. I named this tool the Extract Signatures Tool (EST).

I decided, in order to maximize ease of use, the tool would need to accept a set of points as an input, find the pixel coordinates in the TSI for each point, then extract each point's temporal signature. The average of these signatures could be calculated then written to a file for later use.

To implement this solution, I created a library to read point features from shapefiles, and wrote a function to take the geographic coordinates of each point in a shapefile and convert them into a list of pixel coordinates in a specified image. Next, I wrote a set of functions to read the values of such a list of pixel coordinates and write them to a text file with the format shown in figure

USE A REAL EXAMPLE

. Then, I created a function to find the mean of each date, writing the result to another file. Each of the created files was in plain-text ASII format, and I decided to use the file extension .ref.

Example .ref file
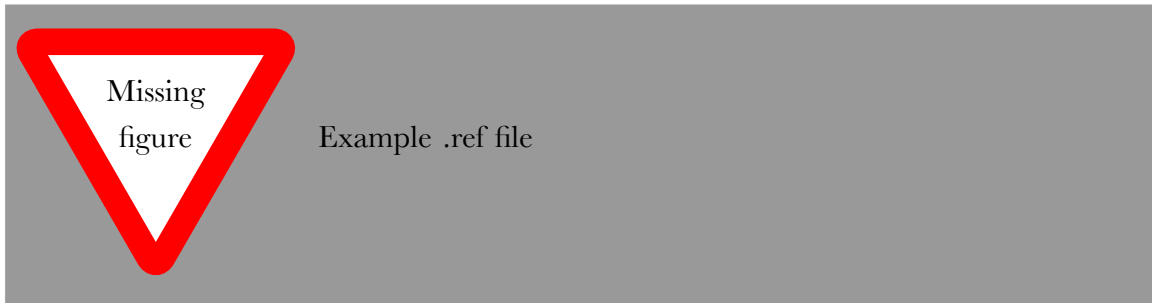
I based the formatting of the .ref files on the .sig files used by ENVI for hyperspectral signatures. Using a plain-text file-based data format currently seems to be the best solution for storing reference signatures, as the data is very simply structured and files are highly portable. However, future implementations of the EST may benefit from a more rigid or better contained data format.

B.4   The Fit Algorithm

Developing the fit algorithm and the corresponding tool was a more complex problem. As described in Chapter 4.3, the basis of the algorithm is Equation 4.3. The equations finds the average difference between a pixel signature and a reference signature (the RMSE), while allowing the reference be transformed within predefined bounds. Minimizing the equation enables the degree of fit between a reference signature and a pixel signature to be quantified. To implement the algorithm, I decided to use scipy's minimize function. I began by building the simplest implementation possible, while making as many parameters as possible into arguments of the enclosing function to allow future testing. I continued building out the functionality until I had a tool capable of reading in a TSI from a file path

and reference temporal signature .ref files in a directory. The tool would then process the TSI using the .ref files, and output a fit raster corresponding to each .ref file.

One clear problem early on was speed. Python's global interpreter lock (GIL), intended to increase the security and reliability of running python code, also has the consequence of limiting code execution to a single processor core. With current multicore processor designs, this prohibits python from using much of the available processing resources. For example, in my eight-core computer, I was limited to using only 12.5 percent of its processing capabilities.

To get around this, I redesigned the tool to allow the use of the python multiprocessing module. With multiprocessing, I was able to spawn a new worker process for each reference signature used (limited to a maximum number of processes as specified by the user), devoting an entire core to processing each fit raster. At first, this seemed to be a great solution: when using five reference signatures, I could find the fit raster in for all five in one-fifth the time. However, the parallel use of resources is not as straightforward as it seems.

In the later stages of testing, I began getting a serious error when attempting to generate fit rasters. I am unsure why the problems began; it may be related to refactoring the code. I know that it had not occurred in earlier testing as the issue resulted in a fatal error, where the program would try to read in a pixel from the TSI and would get a null value. Strangely, this issue would always happen on the twentieth row of the raster. Even stranger, printing the pixel value to the screen would not get a null value, and the program would continue, but careful investigation revealed that the value returned from problem pixels would not be valid (often being zero for every band, or a repeating pattern of negative numbers).

I tried eliminating the parallelism problem by using just a single worker process, meaning only one process would be trying to access the GDAL image object in memory. Preventing concurrent access to that object had the intended effect, and the problem disappeared. I tried using the multiprocessing lock construct to prevent multiple processes from reading the image object simultaneously, but this had no effect. Finally, after reading the multiprocessing documentation yet again, I decided I would try reading the TSI into an array in memory, as arrays seemed to be safer in concurrent applications. With this change, the problem vanished. I still cannot say why this is, as one would think concurrently *reading* memory should not cause a problem. Nonetheless, this was the fix. Additionally, this solution also had the benefit of providing a moderate speed boost, though unfortunately this solution also raises the memory requirements of the program: the entire TSI must be read into memory, and all the output arrays are also in memory, so the memory footprint is roughly equal to $s * (n + 1)$ where s is the size, in bytes, of the TSI image, and n is the number of worker processes.

Other problems I had throughout development were issues involving pixel coordinates. Sometime highly pervasive, these problems stemmed from the fact that arrays use matrix-style coordinates in row-column order, while GDAL functions require coordinates in terms of x-offset and y-offset, which is actually column-row order[2]. One must remain cognizant of which data type with which he or she is interfacing, especially when refactoring involves changing between GDAL image objects and arrays, or vise versa.

Using the algorithm is easy, as it has a command line interface through the Find Fit Tool. Due to the numerous parameters required by the algorithm, the command has many

options. However, it only requires that the user specify the the path to the TSI image, the path to the directory containing the .ref reference signature files, and the start day-of-year and day-of-year interval for the TSI. All of the other options require user input only if the user wants to use a non-default value.

B.5   Creating a Classification From the Fit Rasters

Merely finding the fit rasters does not a classification make. The first step in creating a classification is to find valid fit values; even pixels that are obviously different than a reference signature will result in some measurable fit. Thus, the fit rasters need to be thresholded to eliminate extraneous high values.

Choosing a value at which to threshold the fit rasters is not a simple decision. One can think of the threshold in a similar manner to weighting: a higher threshold will allow more pixels from that fit rasters to be considered in the final classification. The correct threshold for a fit raster will vary depending on a variety of factors, including what types of crops are in the sample area, what crops are trying to be identified, and how homogeneous the pixels for that crop are in comparison to the reference signature used. The extent to which these and other factors influence the optimal threshold is not well understood and requires further study. Despite not knowing the exact effects of these factors on the optimal threshold value, it is clear that the optimal value will vary between fit rasters. That is, a single value used across all fit rasters in a classification is unlikely to provide the highest possible accuracy.

Nonetheless, once the fit rasters are thresholded, one can make a classification by finding

the best fit for every pixel. For example, if, for a given pixel, the thresholded corn fit raster had a value of 356.7, soy had a value of 531.5, and winter wheat did not have a value (as the original fit raster's pixel value was above the threshold limit used), the best fitting signature would be that of corn, and the classification could be assigned a value corresponding to corn. If a pixel did not have a value under the threshold used for any of the fit rasters, then that pixel would not be classified (or could be classified as "other").

In order to automate this thresholding/best fit process, and to provide a means to quickly iterate through possible threshold combinations, I created a command line classification tool called the Classify Tool. The tool requires the user to specify the fit rasters to be classified, a truth raster, and threshold parameters. The threshold parameters allow the user to specify the starting threshold value, the number of threshold steps to test, and a threshold step value (the amount to increase the threshold by for each step). The truth raster is ground truth for the entire classified area, and is assumed to match the fit rasters' pixel grids exactly and cover the same geographic extent (such that every pixel coordinate in the fit rasters and truth raster will describe the same geographic location and extent). From these parameters, the tool will automatically generate every possible threshold combination. Then, the tool will brute force through all of the possible threshold combinations, creating a classification and checking the accuracy of each. The tool will output a classification raster created with the highest accuracy combination, as well as a report detailing every combination tested with a confusion matrix for each.

Appendix C

A Breakdown of all Completed Testing

C.1   Round 1 Testing: Initial Classifications

Testing Considerations

I began testing the tool with three main questions. I wanted to know how the accuracy of classification is affected by:

- The spatial distribution of pixels chosen to create the reference curves.

- The temporal distribution of pixels chosen to create the reference curves.

- The VI used for the classification.

To test these factors, I chose six small sample areas dispersed across Kansas, each 100 MODIS pixels square, or about 2.3 KM^2 (Fig. C.1). Using the USDA CDL as reference, I identified areas containing a mix of corn, wheat, soy, sorghum, and winter wheat pixels. I did my best to distribute the small areas across the state to capture a wide variety of growing conditions. This task was surprisingly difficult, given the large extent of the state and the concomitant variation in growing conditions. The crops favored tended to change from

one area to another; for example, few sites in western Kansas had little more than corn and wheat.

Within each sample site, I found four to eight MODIS pixels of each of the previously listed crop types. I took care to choose only pixels in the center of fields, under the assumption such pixels would be more representative of the crop's true temporal signature. On each chosen pixel, I digitized a vector point feature, keeping points for each crop and study area in separate shapefiles (Fig. C.2). I used these shapefiles as inputs to the RSG, and created two sets of reference temporal signatures for each study area: one set from the NDVI MODIS data, and another from the EVI data. I also found the mean of the signatures identified for each crop in easy study area, which gave me mean NDVI and EVI reference temporal signatures averaged across all six study sites.

I classified both NDVI and EVI data for each of the sample areas using its own reference signatures, the reference signatures derived from each of the other sample areas, and the mean signatures from all of the sample areas. This allowed me to test how the spatial distribution of pixels used to construct reference signatures affects the accuracy of classification, and which of these two VIs performs better. My initial hypothesis was that averaging signatures across multiple sites would decrease the "truthfulness" of the reference signatures because of geographical discrepancies in season start date, maximum VI intensity, and/or season length. If reference signatures are usable between study areas, but averaging multiple sites together does in fact negatively affect the derived reference curves, I expected to see rather consistent classification accuracies independent of the reference signature set used, but that the mean reference signatures produced a lower classification accuracy than

those derived from single sample sites. However, if reference signatures are not useable be-tween study areas, I expected low accuracies when the reference signatures from different study areas are used for classification, while the mean reference signatures should perform somewhere between those of the study area in question and those of the other study areas. If spatial distribution has no effect, my expectations was that the classification accuracies would be relatively consistent no matter which reference signature set is used.

I knew these tests would not directly answer my question about temporal variation in the construction of reference temporal signatures. To get an accurate answer, I knew I would need to repeat the above testing, replacing location with time as the key variable. However, given my hypothesis about the effects of spatial variation, I wanted to find out my results before devising this test. If I found the spatial distribution of pixels negatively affected the classification accuracies, then I could reasonably conclude adding a temporal component would have a similar outcome, as temporal variance would also introduce discrepancies in season start date, maximum VI intensity, and/or season length. In such a case, additional testing of this parameter would not be necessary to proceed.

Round 1 Results and Discussion

Some clear patterns pop out when reviewing Table C.1. First, a quick scan of all the values shows that none of the classifications had a very high degree of accuracy, though study site 3 stands out with much higher accuracies than the rest. A more detailed examination of of study site 3's results shows that the increased accuracy is due to the fact that relatively few of the pixels in the sample site are crop pixels, and a high accuracy can be achieved by not

Graphics/Testing/STUDYSITES.pdf

Figure C.1: The six study sites in Kansas.

classifying the majority of the pixels, such that they are considered "other." A breakdown of

highest accuracy sample site 3 classification, that using sample site 3's reference signatures

and NDVI data, is shown in Table C.2. One can see the relative abundance of "other"

pixels that skews the accuracy upward compared to the other sample sites.

[INCLUDE THE TOP ACCURACIES OF EACH OF THE OTHER SAMPLE

SITES IN TABLES]

Another pattern that stands out is that using NDVI resulted in a higher top accuracy

for every sample site. The numbers are fairly close between the two, so I am hesitant to

conclude that optimizations would fail to make EVI-based classifications as or more accurate

than NDVI-based classifications. Nonetheless, based on these results, I have determined to

Table C.1: Overall Percent Accuracy for Each Round 1 Classification, by Sample Site (SS). Green cells indicate highest accuracy for each SS.

	EVI						
	Reference Signatures Source						
	SS 1	SS 2	SS 3	SS 4	SS 5	SS 6	Mean
SS 1	55.61		45.34	54.36	43.83	49.06	49.63
SS 2	53.11	64.93	50.00	47.86	40.79	42.60	53.69
SS 3	73.87	69.40	75.23	73.53	70.57	71.86	73.71
SS 4	50.42	45.54	49.26	53.46	45.30	49.66	52.54
SS 5	42.05	45.62	56.00	54.68	55.06	49.02	40.29
SS 6	47.78	48.66	38.43	47.53	41.60	49.55	48.44

	NDVI						
	Reference Signatures Source						
	SS 1	SS 2	SS 3	SS 4	SS 5	SS 6	Mean
SS 1	61.08	48.29	47.91	60.72	44.85	51.81	52.75
SS 2	56.08	67.39	42.66	52.59	50.62	48.95	61.21
SS 3	74.88	71.75	78.69	77.16	70.62	71.75	73.70
SS 4	56.30	42.25	46.89	59.21	44.72	54.26	52.48
SS 5	53.57	48.51	45.93	62.18	62.83	60.21	53.07
SS 6		51.90	38.28	49.82	47.15	55.71	54.36

Table C.2: Round 1 Testing: Sample Site 3 Best Accuracy Using NDVI

	Corn	Soy	Wheat	Other	Total	User Accuracy
Corn	861	133	0	334	1328	65%
Soy	28	558	13	198	797	70%
Wheat	2	4	23	37	66	35%
Other	884	424	74	6427	7809	82%
Total	1775	1119	110	6996		
Producer Accuracy	49%	50%	21%	92%		

Overall Accuracy: 79%

Kappa: 0.49

Graphics/Testing/clip1_30mCDL_smpl_old.pdf

Figure C.2: Points dropped on pixels to use for reference signatures in study site 1.

continue testing with NDVI only, as it seems to perform better.

Perhaps most striking pattern in Table C.1 is that, aside from sample site 5 in the EVI-based classifications, the highest accuracies occurred when the reference signatures generated from a particular study site were used to classify that same study site. This is not wholly unexpected—even if temporal signatures are largely location-independent, there is likely to be some location-specific phenomena influencing the shape of the signature curves. In some cases, it appears that some of the classifications using other reference signatures were of similar accuracy, as occurs with sample site 1 when it is classified using sample site 4's signatures (61.1 percent versus 60.7 percent). However, in other cases, the accuracy is marked

lower, exemplified by sample site 1 when it is classified using signatures from sample sites 2, 3, 5, and 6 (all are around ten percent lower in accuracy).

The accuracies of the mean reference signature classifications are generally low. They are never the worst, which may suggest that it is better to average a greater number of pixels together if the representative-ness of the chosen pixels cannot be established. However, this conclusion would support a more selective and refined approach to creating reference signatures: don't try to average out bad pixels, eliminate them in the first place.

Looking back on the scenarios I outlined in my testing considerations above, I actually found none of them completely captured the behavior shown in the results. I did not see relatively consistent classification accuracies independent of the set of reference signatures used, but I also found that the reference signatures from some sample sites did well at classifying others. The mean signatures were also somewhat in the middle, generally not doing terribly well, but sometimes coming close. The best interpretation I could make of the results is that, under the right circumstances, reference signatures can be used to classify other areas. However, the cases where the reference signatures are not portable, in addition to the low overall accuracy levels, were concerning. I began to consider that I might not be able to answer the initial testing questions; instead, I realized I needed to take a step back and better explore what factors effect the classification process.

C.2   Round 2 Testing: Eliminating Mixels

Pre-testing Investigation

I began my Round 2 testing by diving back into my Round 1 results. I wasn't sure exactly what I needed to test, but I knew my previous results held more clues. For the sake of simplifying my investigation, I decided to focus solely on sample site 1 for the remainder of my testing. If I could boost the accuracy of its classification, I would identify some of the factors influential in the classification process. I chose sample site 1 over the others as it has the best variety of crops in which I am interested, and also includes some large non-crop areas of different land cover types. This mix seemed to offer the best testing environment of my six sites.

I first studied the classification results for sample site 1 from Round 1 produced with its own reference signatures (Fig. C.3). I noticed that the major patterns generally matched the CDL fairly well. If the classification *looks* correct, however, where were the errors? Obviously there should be many incorrect pixels, as this classification only had an accuracy of about 61 percent. Yet they weren't obvious at first glance.

To find these incorrect pixels, I created two images: an image with the incorrect pixels masked in black, and an image with the correct pixels masked in black (Figs. C.3c and C.3d). In the former, I noticed that many of the incorrect pixels seemed to fall on the edges of fields. In the latter, I noticed some class confusion, a finding reinforced by the confusion matrix for this classification (Table **??**).

The class confusion seemed to be a problem, but how to begin to remedy it was not im-

Graphics/Testing/clip1_MODIS_CDL.pdf Graphics/Testing/clip1_MODIS_round1.pdf

(**a**) The 2012 CDL.

(**b**) Round 1 classification using SS 1 signatures.

Graphics/Testing/clip1_MODIS_round1_cor/Tes.pdf Graphics/Testing/clip1_MODIS_round1_inc

(**c**) Correctly classified pixels. Incorrect pixels in black.

(**d**) Incorrectly classified pixels. Correct pixels in black.

Figure C.3: Round 1 Testing: Sample Site 1 Classification.

mediately obvious to me. That so many border pixels were incorrectly classified, conversely, suggested to me that this classification method struggles when pixels have more than one land cover. Such pixels are often termed mixels.

The problem with mixels is that each land cover in a mixel has a different temporal signature. The different signatures are aggregated at the pixel level and become mixed, creating a new signature representing that specific mixture of individual signatures. This problem is not unique to my temporal data; all raster land cover data has mixels. Users of spectral data even have spectral unmixing tools to extract subpixel spectral information.

CITATION

In my case, the large size of the MODIS pixels increases their possible effect on classification accuracy. Many different land covers can be included within a 232-meter square. The large pixel size also means that a much greater percentage of the study area is composed of mixels than if a smaller pixel were used.

For these reasons, I hypothesized the low classification accuracy was because mixels could not be processed accurately by the fit algorithm due to the contaminated signal in a mixel curve. In other words, if two crops are mixed within a pixel, the curve of that pixel's values from the time series image will be a blend of both crops' phonological curves, and neither will have a good fit. Additionally, the crop which may occupy the majority of the area of the pixel may not be the largest contributor a pixel's values; for instance, due to its high maximum VI values, a crop like soy may drive a pixel's values up at the time of the year it is mature, even if it is in the minority of the pixel. This would further reduce the accuracy when compared to the CDL resampled by majority. Consequently, I determined I needed

to find a way to removed mixels from the classification.

The Testing Process

The first step in removing the mixels was to extract the MODIS raster grid from the sample site 1 TSI as vector polygons. The CDL raster is of sufficient spatial resolution (30-meter) to allow identification of fields; I converted the CDL to vector, and all continuous pixels of the same land cover value were merged into single vector features. Next, I intersected these CDL features with the pixel polygon features of the MODIS grid. From the resulting vector features I was able to select only those with an area close to that of a full MODIS pixel. Specifically, I decided to select all features greater than or equal to 53,000 m^2 in area (a full MODIS pixel being 53,824 m^2). I also manually added two sorghum pixel features that were not selected via this process because of the low number of sorghum pixels retained. The result, shown in Fig. C.4, was 1,359 features selected. These features can be thought to represent MODIS pixels which have "pure" signatures: each pixel has only one land cover contributing to its temporal signature, so each should be representative of its class.

   To allow me to classify only these pure pixels, I found the centroid of each of the selected pixel polygon features. The subset option of the Find Fit Tool allowed me to specify a shapefile of point features, which were converted to a list of pixel coordinates from the TSI; the tool then found the fit of the pixels in this list only. All the other pixels were assigned the no data value. All other classification steps were the same as in Round 1, except the no data values in the fit rasters were ignored by the Classify tool when considering accuracy.

Graphics/Testing/clip1_30mCDL_pure_pixels.pdf

Figure C.4: Round 2 Testing: Pure pixels in Study Site 1.

Round 2 Results and Discussion

The pure-pixel-only classification is shown in Fig. C.5, and its confusion matrix is Table C.3.

The confusion matrix shows the vast majority of errors are errors of commission in the corn

class. Almost one third of the soy pixels and close to half of the "other" pixels are classified

as corn. That corn and soy have similar signatures may suggest that those crops will always

have some confusion because the similar shape and close maximum dates of early soy and

Graphics/Testing/clip1_MODIS_round2.pdf

(**a**) The classification results.

Graphics/Testing/clip1_MODIS_round2_correct.pdf

(**b**) Correct pixels, with incorrect pixels colored black.

Figure C.5: Round 2 Testing: Classification of Study Site 1 Pure Pixels.

Table C.3: Round 2 Testing: Sample site 1, NDVI, Pure Pixels

		Corn	Soy	Wheat	Other	Total	User Acc.
		Reference Data					
	Corn	358	108	3	79	548	65%
Classified	Soy	10	236	0	11	257	92%
	Wheat	36	6	348	29	419	83%
	Other	10	4	20	101	135	75%
	Total	414	354	371	220	1359	
	Prod. Acc.	86%	67%	94%	46%		

Overall Accuracy: 77%

Kappa: 0.68

late corn are not differentiable to the fit algorithm. However, if this were the issue, I would expect to see the confusion in both directions, with a greater number of corn pixels wrongly classified as soy. That the confusion is mainly one-sided led me to believe this is not the problem. Additionally, that so many "other" pixels were classified as corn suggested to me that the reference signatures I created might not be accurate.

Missing figure

MAKE CSVs OF DATA AND MAKE PLOTS FOR NEXT PARAGRAPH
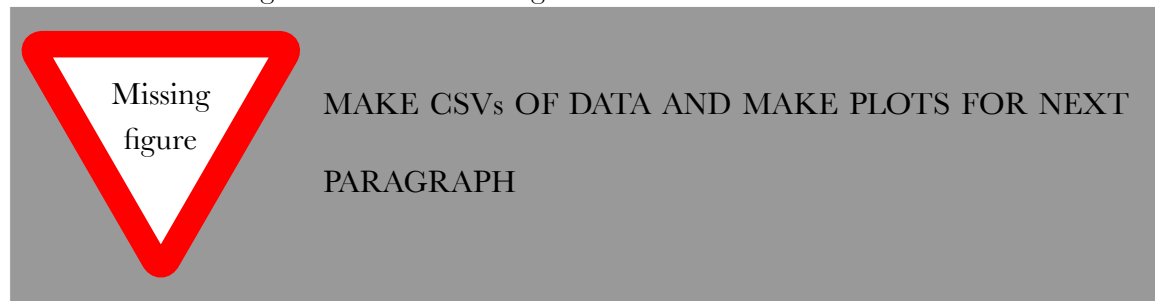
I plotted the signature of each of the pixels contributing to the reference signatures

REFERENCE TO FIGURE

to see what the signatures looked like. Comparing them to the signatures shown in Wardlow and Egbert revealed numerous discrepancies (2005). I decided that I needed to

change my strategy for identifying pixels to use in making the reference signatures. Rather than simply finding pure pixels, I needed to ensure the signatures of sampled pixels were representative of the expected crop signature.

C.3   Round 3 Testing: Refining the Reference Signatures

ENVI has a plotting tool that allows the user to interactively select pixels in a multi band raster and view plots of the pixels' values. This tool proved perfect for refining the reference curves, allowing me to drop points on only those pixels having an appearance matching my expectations for the crop designated by the CDL (see Fig.
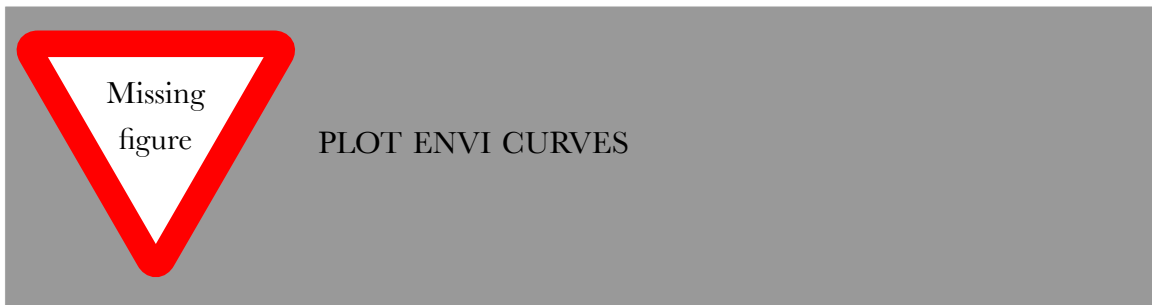
INSERT REF TO FIGURE

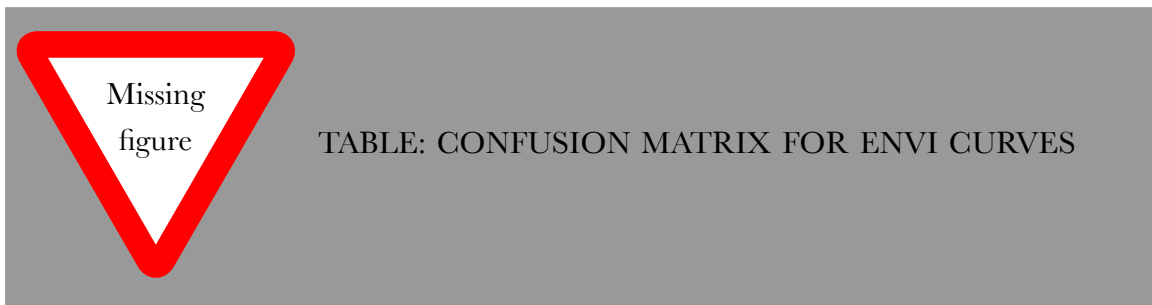) . The new reference signatures, and the signatures of the newly-selected pixels are shown in Figs.

INSERT REFERENCE TO PLOTS

Missing figure

INSERT FIGURE OF NEW AND OLD POINTS FOR REF CURVE GENERATION

Missing figure   PLOT ENVI CURVES

Round 3 Results and Discussion

Missing figure   TABLE: CONFUSION MATRIX FOR ENVI CURVES

To my surprise, I found that refining the reference signatures actually reduced the classification accuracy to 66 percent (Table
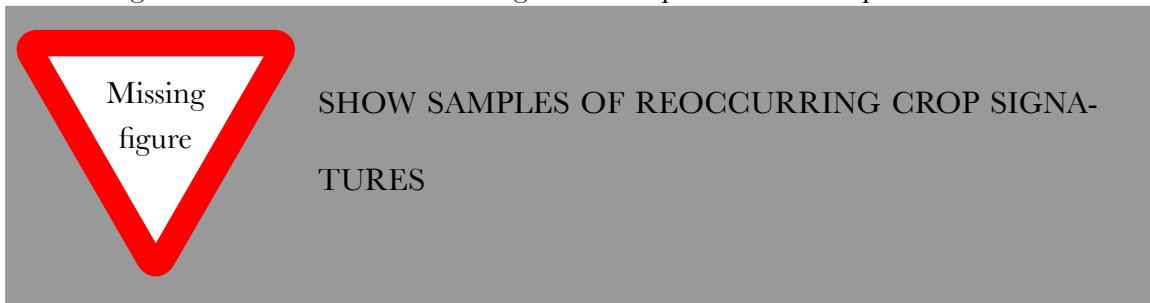
INSERT REFERENCE TO TABLE

). I did notice almost all of the "other" pixels were correctly classified, but also that, in contrast to the Round 2 testing, errors of omission were primarily responsible for the decrease in accuracy. That is, many corn pixels in the study were classified as other. The confusion between corn and soy also remained.

To further understand what had happened, I plotted the signature of every incorrectly classified pixel in the study site. Looking through the plots, I began to notice some patterns.

I found many adjacent pixels with similar plot shapes

> ⚠ Missing figure
>
> SHOW SOME SAMPLES OF ADJACENT PIXEL SIGNA-TURES
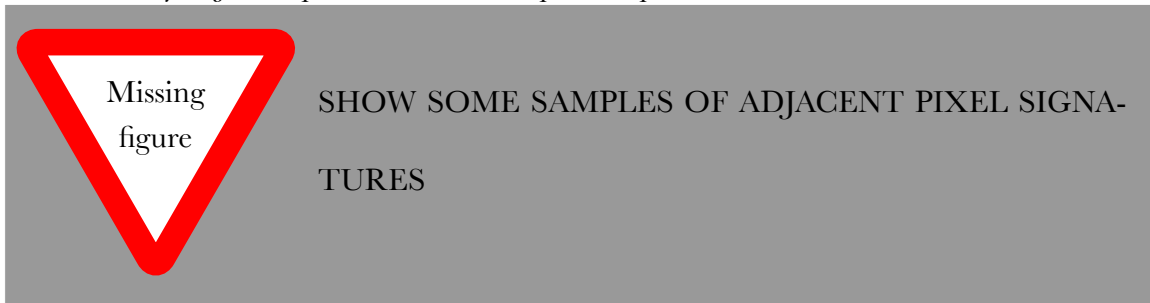
. I also began to notice a few different signature shapes for each crop

> ⚠ Missing figure
>
> SHOW SAMPLES OF REOCCURRING CROP SIGNA-TURES

. These two findings suggested to me that all pixels in a field generally have the same signature, and, assuming the truthfulness of the CDL, each crop has multiple temporal signatures.

The latter of these conclusions was particularly problematic to me. Not only does such reasoning conflict with previous research into phenological classification

> CITE WARDLOW AND EGBERT, OTHER CROP CLASSIFICATION SOURCES

, but is illogical considering the typical growth cycle for crops like corn and soy. The same crops within close proximity should be exposed to essentially equal growing conditions. Variations in planting date may account for slight differences in the temporal signatures. The use of irrigation or application of pesticides, fertilizers, or herbicides may also impart slight disparities between signatures. However, none of these variables would likely be accountable for the vastly different crop signatures observed.

To get an expert opinion, I sent a few sample signatures of incorrectly classified pixels, labeled as corn in the CDL

Missing figure

INSERT GRAPHICS OF THESE SIGNATURES
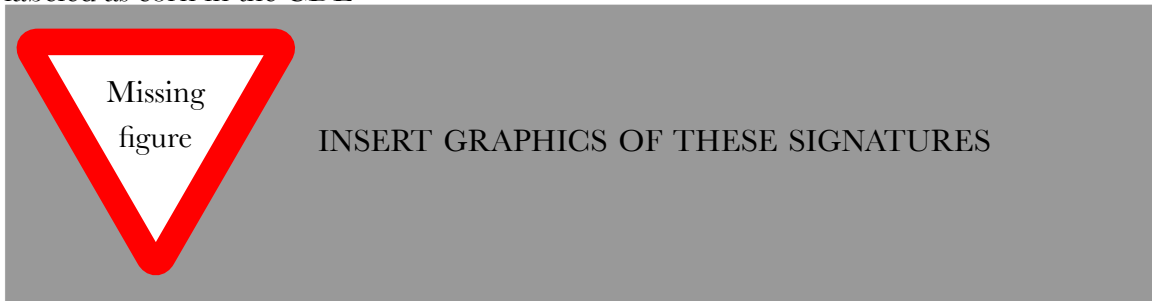
, to Dana Peterson at the Kansas Applied Remote Sensing Program of the Kansas Biological Survey at University of Kansas. Conferring with her and her colleagues confirmed that the signatures could only be attributable to double cropping, and that the CDL is not correct in these cases.

CITE CORRESPONDENCE

Another class class of signatures had an unusual bump in value at the end of the year. The crop signatures shown in Wardlow/Egbert made me think the end-of-year increase in NDVI of many incorrectly classified pixel may be related to winter wheat planting for the next year's growing season.

To investigate this idea, I used the USGS Landsat Look online imagery viewer to identify some of these incorrectly classified fields and see how they appeared through time. The fields with the increase in values at the end of the year featured vegetation throughout the winter, and had significant vegetation growth early in the following year, consistent with winter wheat. Moreover, the CDL for 2013 showed many of these fields to have winter wheat in that year (including both winter wheat/soy double cropping and winter wheat only)

CONFIRM THIS

.

C.4   Round 4 Testing: Different Time Ranges

Deriving the Date Ranges to Test

As many of the pixels this winter wheat bump did not fit the reference signatures within the utilized thresholds, I wondered what would happen if I changed the date range of the TSI. Instead of beginning and ending the TSI at the start of January, I decided to create a TSI that would include the end-of-year winter wheat bump from 2011 and end before the bump in 2012. Specifically, I selected images from 2011 DOY 305 through 2012 DOY 289.

Missing figure

CREATE A MAP OF INCORRECTLY CLASSIFIED SHOWING 2013 WINTER WHEAT PIXELS
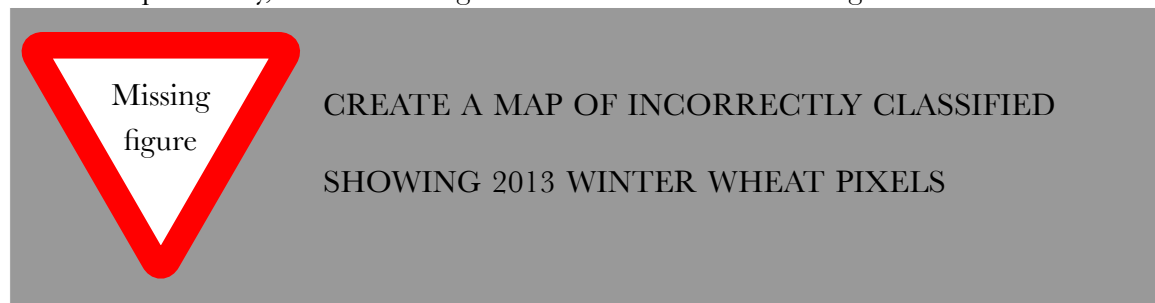
As by this point I had also returned from my field work in Argentina, I had a bit better idea of how my processing procedure would have to change to classify the Pellegrini imagery. In talking with the locals, I found that wheat was just one of a number of different grains that were grown in the winter dry season, and I did not have any good way to verify where nor what types of such crops were grown in the season proceeding my travels (I was there only during the summer season). To compound the problem, I also learned that, due to the length and flexibility of the summer wet season in Pellegrini, farmers were not limited

to double cropping only late summer crops with a winter crop. Instead, any summer crop could be grown with a winter crop. As I was only able to extract one double crop signature from the Kansas data, the winter wheat and soy signature, I realized I would not be able to use my Kansas signatures to classify an entire agricultural year in Argentina; I would only be able to classify summer crops. Because of this, I decided to see what would happen if I limited my sample site 1 classification to only the spring and summer months, using images from DOY 97 through DOY 273.

Classification Procedures

The only difference in the processing procedure for these two classification as compared to the previous procedure in Round 3 was that I selected the desired MODIS .hdf files covering each of the date ranges and placed those files in two folders. I then used those folders as the directories for the MODIS .hdf sources when building the two TSIs. I used the same reference signatures as derived in Round 3, and only classified the pure pixels identified in Round 2.

Round 4 Results and Discussion

Despite accounting for the winter wheat planting for the following year, my 2011–2012 classification was only marginally better than the full 2012 classification, achieving 68.1 percent accuracy
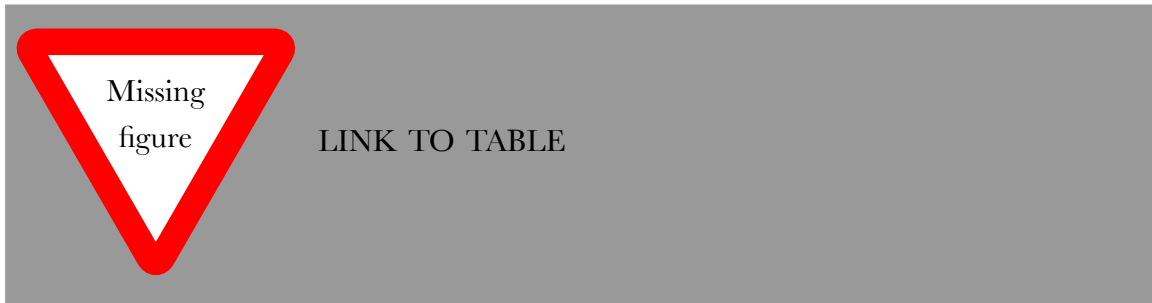
. Looking at the classification, it appears that a few of the winter wheat 2013 pixels were properly classified this time, but many remained incorrect. Evidenced by the percent accuracy, most improvements were offset by pixels now unable to be accurately classified. Given that I knew I would be focusing only on summer crops in Argentina, I did not further investigate why this was the result.

The 2012 summer-only classification fared slightly better. Given the date range, I only classified the three main summer crops—corn, soy, and sorghum—finding an accuracy of 75.1 percent. Looking at the classification and confusion matrix, I realized much of the error was due to confusion between soy and sorghum.

Considering that only 18 pixels in the study area were sorghum, I tried without it, classifying just corn and soy. However, this merely traded confusion between sorghum and soy for confusion between corn and soy, maintaining more or less the same accuracy.

In both summer-only classifications, I did find the accuracy to have increased, but I began to wonder if these results were directly comparable to the previous results, given that I had always been finding winter wheat, corn, and soy. To test this theory, I reclassified the 2011–2012 fit images, looking for the summer crops without wheat. Surprisingly, I found the accuracy to be exactly the same as classifying just the summer months. This is at least

validation that restricting the classification to only the summer months does not have a negative effect on finding the summer crops. Because of this, and my working in Argentina, I decided to use the summer-only approach for all subsequent testing.

C.5   Round 5: A Last Ditch Effort to Match the CDL

This section has outdated results; update as necessary and link to main results and discussion where necessary as this will just be repeated information.

In attempt to create a classification to match the CDL as best as possible, I performed a cluster analysis of the pixels of each of the crops to try to isolate the different signatures I previously identified. To begin, I created multiple masks of the TSI, each to isolate all the CDL full pixels of one of the summer crops or the wheat-soy double crop. The TSI was then processed in ENVI with each of these masks using the k-means unsupervised classifier. Each cluster of a crop represented the different temporal signatures of that crop. I converted each pixel in the resulting clusters to vector points, organized in individual shapefiles by crop and cluster number (i.e corn3.shp is corn cluster 3). Each of these files was used with the reference curve generator tool to provide the coordinates to generate a .ref file of the mean signature for each cluster.

I used the fit tool to generate fit rasters for the .ref files, then fed them into classification/accuracy tool. That the latter tool is designed to search the fit raster names for the crop name it represents meant that using multiple fit rasters for each crop required no modifications to the code. In other words, simply telling the tool to look for "corn", which has a value in the CDL raster of one, allowed each subset to be checked for accuracy not against itself,

but against the greater whole. I determined this would provide a better means of checking the ability of the classification, as k-means might cluster pixels together that could be better fit with another of said crop's curves, due to the difference in the k-means algorithm versus my fitting algorithm (e.g. it is possible that a reference signature could be transformed to fit a pixel signature very well even if the pixel signature looks very different from the reference to the k-means classifier).

I actually ran this processing chain twice using different cluster settings. Due to processing constraints in the classification and accuracy assessment step, I ran the first k-means with three clusters for each crop, a 1.0 percent change threshold, and 100 iterations maximum. I considered using more clusters, but three seemed to be optimal, finding multiple signatures while keeping processing times manageable. Even using only three clusters per crop, four threshold steps, and omitting the wheat-soy double crop reference, the classification/accuracy assessment tool needed over 82 minutes to complete. Adding even one more cluster per crop would have taken almost twenty-two hours to finish.

Using the clusters for did in fact increase the classification accuracy to almost 82.5 percent, as shown in figure

and table
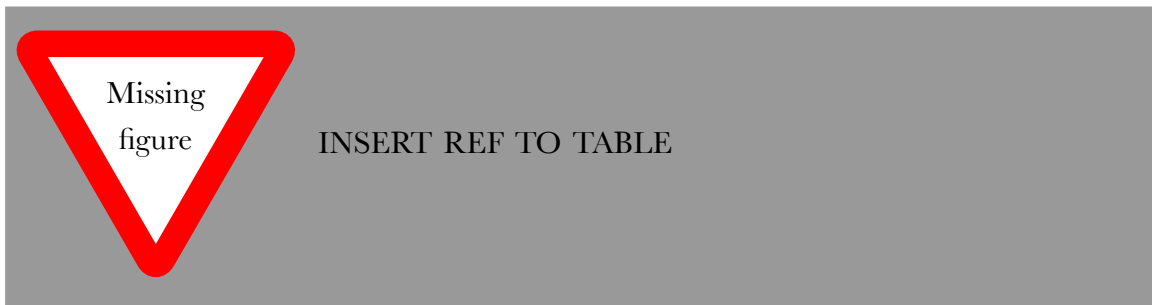
. After reviewing the results, I realized the sorghum was really not adding to the accuracy; omitting the sorghum cluster reference resulted in an ever-so-slight improvement, achieving an accuracy of 82.6 percent. It seems, especially in light of the fact that the CDL does not have clearly-delineated sorghum fields, but rather a mix of soy and sorghum, that the USDA's classification method is unable to accurately differentiate between the two crops. Or, it could be that my method also has difficulty with these crops, given their similar temporal signatures.

One of the soy signatures had a strange, non-soy-like appearance. I decided to re-run the classifier as before, but omitting the peculiar soy signature. The accuracy did drop to 81.5 percent, but when I visually analyzed the classification I could see that all the previous errors where non-crop pixels were classified as soy were no longer present. I interpret these results to mean either that some soy fields have signatures quite similar to grassland and pasture areas, or that the CDL inaccurately classifies some grassland or pasture as soy. From my understanding of crop phenologies, and given my experience looking at crop signatures, I believe the latter is more likely.

When I ran the kmeans clustering a second time, I used ten clusters and 100 iterations. This clustering produced thirty clusters: ten each for corn and soy, nine for wheat-soy double

cropped, and one for sorghum. Processing thirty fit rasters with the classification/accuracy tool using just two threshold values would theoretically take 0.35×2^{30} seconds—almost twelve years—to complete on my computer. Rather than wait for that process to complete, I decided to use a single threshold across all the fit rasters and see what the results would be like, stepping through threshold values of 400 to 850 by increments of 50. The highest accuracy classification, 71.7 percent, occurred at with a threshold of 650 (see Table **??**). Omitting both wheat-containing reference signatures boosted the classification accuracy to 79.2 percent at the same 650 threshold value. A last test without the sorghum signature proved to be the highest accuracy at 81.0 percent, again with the same threshold of 650.

C.6   Discussion and Conclusions

Are the results still rather low because the CDL has class confusion? That is, might my inaccuracy be compounded because of inaccuracies in the CDL that my classification methods will never recreate? I must posit that my method might actually be more accurate than I can test given the problems with the CDL. However, even if the accuracy of the CDL is 90 percent, as is published, what is the a reasonable accuracy for me to achieve? If my classification were 100 percent accurate, comparing it to the CDL would only result in 90 percent accuracy. Thus, a classification of 80 percent accuracy may indeed be higher relative to the actual ground conditions. Only further testing with confirmed ground truth can really say.

Appendix D

Ideas for Future Testing

Given the practical constraints of this particular project, many aspects of this approach to classification have gone largely or completely untested, and some could have a profound impact on the classification accuracy. I am sure that I have not thought of everything that could be tested or improved, but I have compiled the following list of ideas to help future researchers working with these tools, broken down by each step of the workflow, with general ideas at the end. I have included comments where applicable.

D.1 Reference Temporal Signatures

Idea: How does spatial and temporal variation in the sources used to generate a temporal signature (e.g. multiple sample sites and multiple sample years, respectively) effect the accuracy of classifications produced with that signature?

Comment: This question is one that I initially asked and tried to investigate. My findings (presented in

LINK TO SECTION

), were largely inconclusive due to the numerous problems I have identified. Now that I have refined the method somewhat, this question could be revisited. My hypothesis remains the same: the greater the variations averaged together to create a reference signature, the further that signature gets from an ideal reference which can be transformed effectively to fit pixels of that crop.

Idea: Given the previous question, would another method for combining the signatures of two pixels would be more effective when creating a reference signature?

Comment: I have used two methods to average individual pixel crop signatures. The first, used throughout the work presented in the rest of this thesis, is a simple mean of the values at any given date.

I have also tried using a method something like "fit averaging": using the same function as is used to find the fit values for each reference signature, the time shift and horizontal and vertical differences between two signatures can be found. Dividing each of those transformations by two and applying them to one of the original signatures theoretically creates a new signature halfway between the two original signatures. However, in practice, this resulted in strange curve forms when the signatures averaged were not very similar. It may be that this method deserves a second test using the refined sample points, which all have similar shapes, as this approach may be particularly sensitive to outliers. It could also be that I my program to perform this

function has errors.

On the subject of outliers in reference signature generation, it may also be worthwhile to test how using a geometric rather than arithmetic mean of the sampled pixels' values might alleviate the effect of outliers.

D.2   Mixels

I am sure brighter minds than mine could come up with better ways to deal with mixels rather than my simple elimination. For instance, perhaps some method of signature unmixing could allow for sub-pixel classification. With the current process of eliminating all mixels, I do have a few ideas to be tested:

Idea: What is the purity threshold before a mixel is too mixed? That is, what percentage of a whole pixel can still be accurately classified?

Comment: In my case, I, perhaps arbitrarily, chose to eliminate all pixels less than 98 percent of a whole MODIS pixel. This allowed me to select just a few more pixels to classify, presumably without any negative impact from the possible two percent mixing in those extra pixels. Yet, perhaps I could have chosen much more mixed pixels, or should not have chosen pixels mixed even in the slightest. Finding the percentage threshold where classification is still effective is a key step in making this method more useful.

Idea: Do all land covers contribute equally to the temporal signature of a mixel, or do some

land covers have a greater influence on the signature of a mixel? Might the percent mixed threshold discussed above vary depending on the land covers contributing to a mixel's signature?

Idea: Could the classification be used with higher spatial resolution data in such a way to combine the strengths of this classification method with the ability of higher-resolution data to distinguish smaller features? One example of such a method might be to use this process with a low threshold on the fit rasters to identify only fields that have a very high probability of being a given crop. Then, those fields could be used in a standard supervised classification process as training sites, much in the same way unsupervised classifiers are used to generate training sites for supervised classifiers.

Comment: This is one of my favorite ideas, and I am very excited about the potential of combining data and techniques like these. I sincerely hope that someone (perhaps myself) will try this idea. I have high expectations for such a combination. Not only would this idea allow for higher spatial resolution classifications to be made, but would also not require the current thresholding step nor ground truth to create a classification.

D.3   The Fitting Process

Idea: How do the bounds on the transformation coefficients change the performance of the algorithm?

Comment: Loosening the bounds on the transformation coefficients would allow a refer-
ence temporal signature to better fit pixel signatures which are more dissimilar, but
could allow greater confusion between the classes, and could allow reference signa-
tures to fit wholly-unrelated pixel signatures with a low RMSE. Tightening the bounds
would restrict the signature transformation, and may reduce confusion, but could also
prevent the algorithm from fitting reference signatures to legitimate pixel signatures,
resulting in errors of omission. The bounds as used in my testing were determined
almost arbitrarily, being the result of limited preliminary testing and setting them to
something that seemed like it worked. I am certain this is one aspect of the tool that
requires further optimization and has a large effect on classification results.

Idea: What is the best VI for use with this method?

Comment: From my results I believe NDVI is better suited for use with this method than
EVI, the other MODIS-supplied VI. However, many other VIs could be used, and
may allow for better accuracy or different use cases.

Idea: How does the mean used to calculate the RMSE change the classification accuracy?

Comment: Based on the advice of my advisor, I tried using a geometric mean for the cal-
culation of the RMSE in the fit algorithm. With this approach, equation 4.3 becomes:

$$RMSE = \left[\left[\prod_{x=j(1),j(2)\ldots}^{n} \left(f\left(x\right) - g\left(x\right) \right)^2 \right]^{\frac{1}{2}} \right]^{\frac{1}{n}} \tag{D.1}$$

I found it to be too insensitive and it resulted in unrealistically low fit values. It seemed
this mean allowed reference signatures to fit to pixels that should not be classified (they

are "other") in a similar threshold range to pixels which are legitimate. However, with other optimizations to the overall classification process, there may be valuable in formally testing this mean. The Find Fit Tool already has an option to use a geometric mean instead of an arithmetic mean, so this does not require implementation to test.

Idea: Is this the right way to go about comparing a reference signature to an unknown pixel's signature? Would another comparison method be more effective and/or efficient?

Comment: I only pose this question in case someone else might have a better idea than me.

ADD INFO ABOUT OTHER ALTERNATIVE PROCESSES, SUCH AS BOOKMARKED IN THESIS FOLDER...DTW, PROSCRUSTES ANALYSIS, ETC...

D.4   Thresholding and Classification

The thresholding and classification step is the part of this process I dislike the most. My original intention was to create a method for classifying crops without ground truth, but this part of the process requires ground truth to

Idea: How much difference do different thresholds for each crop really make in the overall accuracy? If everything else is optimized, can a single threshold value be used for all the fit rasters without sacrificing much accuracy.

Comment: Understanding if this is a viable alternative is likely necessary if the method is to be used with no ground truth as desired.

Idea: Do the optimal thresholds vary little, or are they highly variable?

Comment: While I have not been testing this formally, the wide spread of the optimal thresholds that I've identified across all my classifications suggests that the best threshold values are unique to every circumstance and quite variable.

Idea: Is there a faster way to iterate through the many possible thresholds than brute force?

Comment: One challenge in the thresholding process is that I have observed local maxima in the classification accuracy. In other words, the accuracy may peak with a certain threshold combination, but that peak may only be a local maxima, and a different threshold combination may allow an even higher accuracy.

Idea: Might the variation within the fit values for a signature contain useful information that could be used to find an optimized threshold value statistically?

Comment: This connects with the previous question. Additionally, if the thresholds could be determined statistically, then no ground truth would be needed to create the classification.

Idea: If multiple signatures are used for a single crop, each resulting in a separate fit raster, should the fit raster for that crop be combined before thresholding using the lowest value for each pixel?

Comment: Barring the realization of a new method for thresholding the fit rasters, this question deserves some thought. Processing time increases exponentially with each additional fit raster. Taking the minimum value from a collection of rasters takes a negligible amount of time. Therefore, if all the fit rasters for a single crop were of equal validity, this would make sense. However, if some of the reference signatures used were not reliable or potentially inaccurate, one would want the thresholding process to eliminate the fit rasters of any such signatures by holding them at low thresholds. Preempting the thresholding process by merging the fit rasters of a signature would not allow the thresholding to weigh the fit rasters unequally.

Idea: Can the classification tool also generate a confidence raster, and if so, would it be meaningful? See

> REFERENCE IDRISI DOCUMENTATION ABOUT CONFIDENCE SCORES

for more details.

D.5   General Ideas

Idea: How does the interval of the imagery (number of images used for a given time period) change the effectiveness of the classification? Does using more images (an interval of less than 16 days) allow for a more accurate classification, or for the use of smoothing techniques on the pixel data to help eliminate noise?

Comment: Sakamoto et al. (2010), whose work has directly informed my own, used the

8-day MODIS composite images, rather than the 16-day composites, which they re-sampled to 5-day intervals to get even more detailed data. They also used a wavelet filter on the pixel curves to reduce extraneous noise. I have been operating under the untested assumption the 16-day composites are sufficiently detailed for this analysis, but that may not be the case. The significant advantage of the 16-day composites, however, is that they do not require much preprocessing. 8-day composites are more likely have cloud cover, and are only available as separate bands, not as preprocessed VIs. If such processing were necessary, it could be automated, but would still be additional complexity. Daily data is also available, but that would further increase complexity, as well as significantly increase storage and memory requirements.

Idea: What about using this method with something other than VI data? What if this could be used multi-dimensionally, with multiple bands? With different data, e.g. higher spatial resolution data, what could be other applications of this method?

Comment: I don't have any use cases in mind when I ask this question. I merely pose it in an attempt to spark an idea for anyone working with different applications.

D.6   Concluding Remarks

The testing I've completed has largely been to demonstrate that the tools I have developed to perform this type of classification are functional and that this hypertemporal signature-fitting approach may be effective for certain remote sensing applications. As one can see by the list above, a lot of work remains to increase the understanding of how different parameters affect

fitting and classification. This study is just the beginning of a large body of potential research, which I believe will only be of increasing importance as earth-observing sensors become more numerous and high spatial and temporal resolution data become more commonplace.

Notes

Chapter 3. Study Areas

[1]The Pellegrini boundary shapefile I obtained does not accurately reflect the bounds of the department on the ground. Particularly along the lengthy and straight northwestern edge, careful inspection of Figure 1.1 reveals a lack of registration between the vector geometry and the obvious boundary visible in the background image. When investigating some of my sample points along the northern and southern edges, I got strange looks and comments about how this or that field was not within Pellegrini, my supposed study area. So with this note, I want to acknowledge that I realize my study area is not actually the Department of Pellegrini proper, but an inaccurate representation as defined by the shapefiles from the Internet. I use this inaccurate representation to ensure consistency, to allow repeatability, and to simplify spatial analysis.

Chapter 4. Data and Methods

[1]For those interested in working with MODIS data, the web address of LPDAAC is https://lpdaac.usgs.gov/, though data is not directly available from their servers without an exact link. I found the best tool for searching the available data was NASA's Reverb|Echo web tool, at https://reverb.echo.nasa.gov/. Using this tool, one can get a list of links in a text file, and can use wget or curl to bulk download the files in the list.

[2]Though the literature typically denotes MODIS data as 250-meter, the composite vegetation indices are actually 231-meter. However, to stay consistent with conventions, I will refer to the data as 250-meter.

[3]Following this pattern exactly will make the first image from the following year be from January 4, but the MODIS composite numbering "resets" at the end of each year. Thus the image interval at the end of the year is shortened, allowing the next image to be produced January 1, though it still covers the proceeding 16 days.

[4]Given the existing literature about phenological classification, I do not believe crops have multiple signatures. I believe every crop as a theoretical ideal signature, which can be made to fit any actual signature using the $xscale$, $yscale$, and $tshift$ transformations in Equation 4.5, barring any unusual effects of weather or other forces impacting crop development (a mid-season drought, for example, may cause a crop signature with double peaks due to the partial dying off and regeneration of the plants). However, given my choice of the CDL as my source of ground truth, I have had to make the assumption that it is highly accurate, despite any evidence to the contrary (see my discussion of the CDL beginning in

Appendix C.3). Therefore, I use the clustering to derive the signatures that will create a classification most comparable to the CDL.

[5]I have not formally tested other bounds. See Appendix D.3.

Chapter 5. Results

[1]NDVI and EVI range between -0.2 and 1.0, so the RMSE values should be 0.0175 or 0.3000. However, the MODIS VIs are distributed as 16-bit signed integer rasters; to allow the VI values to be recorded with such a format, they are multiplied by 10,000, hence the values shown here. I chose not to convert the measurements back to the proper decimal values to simplify processing, though the tools I developed should work either way. Users must take the responsibility be aware of the significance of the fit values and understand what values to expect based on their input data.

Appendix A. The Story of My Field Work

[1]I was tempted to print these double sided to save paper, but decided against it because I wanted to use the back sides for notes. However, it turned out, I did not write many notes, but I was constantly moving the maps around in the binder, and having two attached front and back would not have worked well. So, if anyone uses this idea, do not print double sided, and do not feel guilty about it.

[2]Pellegrini has so many cops; at times it seemed like every other person in town was a cop. Though I don't know if all these people were police, many were in plain clothes and simply walked in off the street

[3]Cultural differences were not helpful in this regard; everyone is extremely laid back; it felt as though few understood the time constraints of my work. However, I even found myself with such an attitude, most likely because of the effects of siestas and eating dinner well into the night; it is hard to get much done after midday. Additionally, the food was generally not my favorite. A lack of calories and sleep conspired to keep my energy levels depressed, so I was often content just to sit around and abide the relaxed atmosphere. Under other circumstances, I would have greatly appreciated this un-busyness. The constant assault of work is, I believe, a severe plight of the American culture, and the Argentine contentedness with leisure is refreshing. Under the looming pressure of a thesis, however, the inability of this environment to foster progress becomes problematic, and increased my stress levels.

Even when I was full of energy and vigor and wanted to get things done, I was often unable to do so, because of my reliance on others who were often occupied. While I felt as though I was not doing enough, I believe they felt like they and I were doing too much. Near the end of my trip, with unfinished work looming before me, I was often told that I needed to stop stressing and relax, yet the relaxing was exactly the cause of my stress! Of course they were right though, as everything was finished in time, thank in no small part to all those who worked to help me complete my project.

[4]Even the simple—and apparently not universal—act of knocking on the door when visiting someone's home: what is one to do when fences, dogs, and sometimes the absence of a front door prevents knocking? Clap of course. While clapping seems an entirely logical course of action after the fact, it was not initially obvious to me, and I found my ability to collect data severely limited until I understood this, and a few other, basic rules and customs

regarding social interactions.

Appendix B. Developing the Processing Tools

[1]Which, quite honestly, is probably not that easy for most, but should be manageable for anyone with command line experience.

[2]One piece of advice to anyone developing raster tools: do not use square test rasters. Doing so hides many such bugs. For example, if the pixel coordinates are accidentally supplied in row-column format when a function is expecting column-row order, a square image will never throw an error, whereas a rectangular image will result in an error when the index of the array is out of bounds. Many otherwise subtle programming errors can be caught this way.

References

Altieri, M. A., and W. Pengue. 2006. GM soybean: Latin America's new colonizer. *Seedling* (Jan.): 13–17.

Boletta, P. E., A. C. Ravelo, A. M. Planchuelo, and M. Grilli. 2006. Assessing deforestation in the Argentine Chaco. *Forest ecology and management* 228:108–114.

Bonnie, R. 2000. Counting the cost of deforestation. *Science* 288 (5472): 1763–1764.

Brown, J. C., W. E. Jepson, J. H. Kastens, B. D. Wardlow, J. M. Lomas, and K. P. Price. 2007. Multitemporal, moderate-spatial-resolution remote sensing of modern agricultural production and land modification in the Brazilian Amazon. *GIScience & Remote Sensing* 44 (2): 117–148.

Clark, R. N., G. A. Swayze, K. E. Livo, R. F. Kokaly, S. J. Sutley, J. B. Dalton, R. R. McDougal, and C. A. Gent. 2003. Imaging spectroscopy: Earth and planetary remote sensing with the USGS Tetracorder and expert systems. *Journal of Geophysical Research* 108 (E12): pages. Available at: http://speclab.cr.usgs.gov/PAPERS/tetracorder/ (last accessed: 11 Aug. 2014).

Exelis Visual Information Solutions. 2013. Selected Hyperspectral Mapping Methods. *ENVI Classic Tutorial.* Available at: http://www.exelisvis.com/portals/0/pdfs/envi/mapping_methods.pdf (last accessed: 12 Aug. 2014).

Gasparri, N. I., and H. R. Grau. 2009. Deforestation and fragmentation of Chaco dry forest in Northwest Argentina. *Forest ecology and management* 258 (6): 913–921.

Geist, H. J., and E. F. Lambin. 2002. Proximate causes and underlying driving forces of tropical deforestation. *BioScience* 52 (2): 143–150.

Grau, H. R., T. M. Aide, and N. I. Gasparri. 2005. Globalization and soybean expansion into semiarid ecosystems of Argentina. *AMBIO: A journal of the human environment* 34 (3): 265–266.

Grau, H. R., N. I. Gasparri, and T. M. Aide. 2005. Agriculture expansion and deforestation in seasonally dry forests of Northwest Argentina. *Environmental conservation* 32 (2): 140.

———. 2008. Balancing food production and nature conservation in the neotropical dry forests of northern Argentina. *Global change biology* 14 (5): 985–997.

Greenpeace International. 2005. The expanding soybean frontier: Argentina's dangerous reliance on genetically engineered soybean. *Greenpeace briefing* (Jan.). Available at: http://www.greenpeace.org/international/Global/international/planet-2/report/2005/11/the-expanding-soybean-frontier.pdf (last accessed: 27 Oct. 2013).

Greenpeace Argentina. 2013. Ley de Bosques: 5 años con pocos avances (Jan.). Available

at: http:

//www.greenpeace.org/argentina/Global/argentina/report/2013/bosques/Ley%20de%

20Bosques.%205%20a%C3%83%C2%B1os%20con%20pocos%20avances%20FINAL.pdf

(last accessed: 2 Apr. 2013).

Gu, Y., J. F. Brown, T. Miura, W. J. Van Leeuwen, and B. C. Reed. 2010. Phenological

classification of the United States: A geographic framework for extending multi-sensor

time-series data. *Remote sensing* 2 (2): 526–544.

Gulezian, S. E. 2009. Environmental politics in Argentina: The Ley de Bosques. Honors

thesis, University of Vermont.

Houghton, R. A. . A. 1994. The Worldwide Extent of Land-Use Change. *BioScience* 44 (5):

305–313.

Huete, A., K. Didan, T. Miura, E. P. Rodriguez, X. Gao, and L. G. Ferreira. 2002.

Overview of the radiometric and biophysical performance of the MODIS vegetation

indices. *Remote sensing of environment* 83 (1): 195–213.

Instituto Nacional de Estadística y Censos. 2010a. Provincia de Santiago del Estero,

departamento Pellegrini: Población total por sexo e índice de masculinidad, según

edad en años simples y grupos quinquenales de edad, año 2010 [Department of

Pellegrini, Santiago del Estero Province: Total population, sex, and index of

masculinity, by age in single years and groups of five]. *Censo nacional de población, hogares*

y viviendas 2010. Available at:

http://www.censo2010.indec.gov.ar/CuadrosDefinitivos/P2-D_86_133.pdf (last accessed:

14 May 2013).

Instituto Nacional de Estadística y Censos. 2010b. Provincia de Santiago del Estero:

Población total por sexo e índice de masculinidad, según edad en años simples y

grupos quinquenales de edad, año 2010 [Santiago del Estero Province: Total

population, sex, and index of masculinity, by age in single years and groups of five].

Censo nacional de población, hogares y viviendas 2010. Available at:

http://www.censo2010.indec.gov.ar/CuadrosDefinitivos/P2-P_Santiago_del_estero.pdf

(last accessed: 14 May 2013).

Masialeti, I., S. Egbert, and B. D. Wardlow. 2010. A comparative analysis of phenological

curves for major crops in Kansas. *GIScience & remote sensing* 47 (2): 241–259.

Pengue, W. A. 2005. Transgenic crops in Argentina: The ecological and social debt.

Bulletin of science, technology & society 25 (4): 314–322.

Price, J. C. 1994. How unique are spectral signatures? *Remote Sensing of Environment* 49 (3):

181–186.

Sakamoto, T., B. D. Wardlow, A. A. Gitelson, S. B. Verma, A. E. Suyker, and

T. J. Arkebauer. 2010. A two-step filtering approach for detecting maize and soybean

phenology with time-series MODIS data. *Remote sensing of environment* 114 (10):

2146–2159.

Sakamoto, T., M. Yokozawa, H. Toritani, M. Shibayama, N. Ishitsuka, and H. Ohno.
2005. A crop phenology detection method using time-series MODIS data. *Remote
sensing of environment* 96 (3-4): 366–374.

Sala, O. E., F. S. Chapin, J. J. Armesto, E. Berlow, J. Bloomfield, R. Dirzo,
E. Huber-Sanwald, L. F. Huenneke, R. B. Jackson, and A. Kinzig. 2000. Global
biodiversity scenarios for the year 2100. *Science* 287 (5459): 1770–1774.

Secretaría de Ambiente y Desarrollo Sustentable [Argentina]. 2007. Informe sobre
deforestación en Argentina [Bulletin on deforestation in Argentina]. Available at:
http://www.ambiente.gov.ar/archivos/web/UMSEF/File/deforestacin_argentina_v2.pdf
(last accessed: 29 Oct. 2013).

Secretaría de Desarrollo Sustentable y Política Ambiental [Argentina]. 2001. *Primer
inventario nacional de bosques nativos [first national inventory of native forests]*. Available at:
http://aplicaciones.medioambiente.gov.ar/archivos/web/UMSEF/File/PINBN/nueva_
version_manuales/pinbn_manual_cartografia_sig.pdf (last accessed: 13 May 2013).

Secretería de Ambiente y Desarrollo Sustentable [Argentina]. 2012. Monitoreo de la
superficie de bosque nativo de la República Argentina, período 2006-2011: Regiones
forestales Parque Chaqueño, Selva Misionera, y Selva Tucumano Boliviana
[Monitoring of the land cover of the native forests of the Argentine Republic, Period
2006-2011: Forest regions of the Chaco, Misionera Forest, and Tucumano-Boliviana
Forest]. Available at: http://www.ambiente.gov.ar/archivos/web/UMSEF/file/LeyBN/
monitoreo_bn_2006_2011_ley26331.pdf (last accessed: 27 Oct. 2013).

Senay, G. B., J. G. Lyon, A. D. Ward, and S. E. Nokes. 2000. Using high spatial resolution multispectral data to classify corn and soybean crops. *Photogrammetric Engineering & Remote Sensing* 66 (3): 319–327.

US Department of Agriculture. 2013. Crops: Kansas agricultural statistics. *USDA national agriculture staticstics service monthly crop production reports* (Jan.). Available at: http://www.nass.usda.gov/Statistics_by_State/Kansas/Publications/Crops/Production/ 2013/cropjan.pdf (last accessed: 25 Nov. 2013).

US Foreign Agricultural Service. 2013. World agricultural production. *World agricultural production circular series* (Apr.). Available at: http://www.fas.usda.gov/psdonline/circulars/production.pdf (last accessed: 27 Oct. 2013).

Valpreda, J. R. 2012. The protection of natural forests in Argentina: Effective actions or words on paper? *INK-ideas, numbers, and knowledge* 1 (1). Available at: http://ink-journal.com/index.php/ink/article/view/9#.Unr-s5TF2fu (last accessed: 6 Nov. 2013).

Volante, J. N., H. P. Paoli, A. R. Bianchi, Y. E. Noe, and H. J. Elena. 2005. Análisis de la dinámica del uso del suelo agrícola del noroeste Argentino mediante teledetección y SIG. Período 2000-2005. [Analysis of the dynamics of the use of agricultural land in Northwest Argentina using remote sensing and GIS. Period 2000-2005.] Available at: http://inta.gob.ar/documentos/analisis-de-la-dinamica-del-uso-del-suelo-agricola-del- noroeste-argentino-mediante-teledeteccion-y-sig.-periodo-2000-

2005/at_multi_download/file/Analisis_de_la_dinamica_del_uso_del_suelo.pdf (last accessed: 13 May 2013).

Wardlow, B. D., and S. L. Egbert. 2002. Discriminating cropping patterns for the US Central Great Plains region using time-series MODIS 250-meter NDVI data–Preliminary results. In *Pecora 15 and land satellite information IV conference,* 10–15.

———. 2005. State-level crop mapping in the US Central Great Plains agroecosystem using MODIS 250-meter NDVI data. In *Pecora 16 symposium,* 25–27.

———. 2008. Large-area crop mapping using time-series MODIS 250m NDVI data: An assessment for the U.S. Central Great Plains. *Remote sensing of environment* 112 (3): 1096–1116.

Wardlow, B. D., S. L. Egbert, and J. Kastens. 2007. Analysis of time-series MODIS 250m vegetation index data for crop classification in the U.S. Central Great Plains. *Remote sensing of environment* 108 (3): 290–310.

Zak, M. R., M. Cabido, and J. G. Hodgson. 2004. Do subtropical seasonal forests in the Gran Chaco, Argentina, have a future? *Biological conservation* 120 (4): 589–598.

Zhang, X., M. A. Friedl, C. B. Schaaf, A. H. Strahler, J. C. Hodges, F. Gao, B. C. Reed, and A. Huete. 2003. Monitoring vegetation phenology using MODIS. *Remote sensing of environment* 84 (3): 471–475.